A PHOTOELECTRIC STUDY OF LINE INTENSITIES IN THE IRON ARC SPECTRUM

Thesis by
Ray Alden Hefferlin

In Partial Fulfillment of the Requirements
For the Degree of
Doctor of Philosophy

California Institute of Technology
Pasadena, California
1955

ACKNOWLEDGMENTS

To the encouragement and guidance of Dr. R. B. King belongs much of the credit for the completion of this work.

I should like to thank Dr. J. L. Greenstein for his assistance on theoretical aspects of the problem.

It is also a pleasure to acknowledge the fine work of Mr. Glen Sligh in construction of the photocell carriages, and the helpful consultations with the engineering staff of the Brown Instrument Division of Minneapolis-Honeywell Regulator Company, Los Angeles.

Finally, I wish to express my gratitude to the California Institute of Technology for the financial help awarded during the past four years.

ABSTRACT

Measurements were made on the 5-meter Paschen-Runge spectrograph with a photoelectric photometer. Special carriages were designed to keep the photocells focused and properly aligned with the grating while the spectrum is scanned. The circuit of the photometer is of an AC ratio type, and the ratios of the intensities of the scanned iron arc lines are recorded automatically by a Brown Recorder.

The temperature and self-absorption present in different parts of the arc, and in the arc under different operating conditions, have been determined with this apparatus.

No self-reversal was observed in the iron arc lines; if present, it was covered by deviations from the values, calculated on the basis of equilibrim considerations, of the intensities of all lines within a multiplet. These variations are different for different multiplets. The possibility that the effect is due in part to systematic error is recognized and discussed, but it appears that the remainder of the effect is due to some mechanism in the arc. Corrections are applied to f-values given in the literature.

TABLE OF CONTENTS

SUPPLEMENTARY MATERIAL

I. INTRODUCTION

This experiment explores the feasibility of using the DC iron arc as a source of excitation for the measurement of f-values of lines in the neutral iron spectrum. It is an attempt to find values of the excitation temperature of the arc, and determine the effects of self-absorption and self-reversal of lines which occur in the arc, over a range of currents and pressures and in several parts of the arc.

A number of atomic f-values, relative and absolute, have been determined by the method of total absorption by King, references (1) to (4); emission f-values determined to 1946 at Utrecht are compiled by Smit (5); f-values found in a large variety of ways are listed by Korf and Breit (6), Unsöld (7), and Aller (8). Each of these authors gives a bibliography.

Such f-values are of more than theoretical interest. They have been used in the study of power arcs (9) and of the internal combustion engine (10); and they allow refinement of the methods of chemical spectroanalysis--(11) and (12). The most intensive application of laboratory-observed f-values has been in astrophysics, where the development of the curve of growth method has yielded copious information about the physical conditions and chemical constitutions of

astronomical objects--for instance see (3), (14), and (15).

Until recently the f-values available have been, due to the limitations imposed by the means of measurement, restricted to transitions of quite low excitation. Thus, the measures of f-values of lines of Fe I by King included none of the weak, high level lines which lie on the linear part of the solar curve of growth.

The use of some astronomical curve of growth to determine f-values for lines of higher excitation--e.g. Wilson (15)--is jeopardized by effects such as the odd-even effect found by Carter (16). Carter succeeded in measuring the f-values of some high excitation lines by producing an emission spectrum of iron in a furnace.

The arc is well known to emit lines of higher excitation than the furnace, and it was thought that the arc might provide a convenient source for extending the list of lines for which f-values are available.

The theoretical background is that of simple emission line theory, extended by Cowan and Dieke (17) into a definitive analysis of the type of behavior to be expected of lines emitted by an arc.

The lines were observed with a twin photocell photometer. The photometer records the instantaneous ratios of the lines observed by the photocells. The spectrograph is a Paschen-Runge type with a horizontal circle 5 meters in diameter.

Over a large part of the Rowland circle are mounted steel rails, and special carriages for the photocells were designed and built which allow scanning of the spectrum. The arc runs vertically inside the vacuum chamber, which is used also for the arc at atmospheric pressure as a wind shield. Light passes out through a window and is focused by a lens onto the vertical spectrograph slit. Shortening of the slit by a mask permits the use of light from only a small part of the arc at one time; and thus it is possible to study the phenomena of interest in different regions of the arc, as well as under different conditions of current and pressure.

II. THEORY

A. Elementary Theory of the Emission Line

The classical emission line theory is presented in numerous sources, for instance Richtmeyer and Kennard (18). A classical electron radiates, due to accelerations in its trajectory, an amount of energy per second

$$\frac{dW}{dt} = \frac{16}{3}\frac{\pi^4 \nu^4 e^2 a^2}{c^3},$$

where a is the amplitude of the (damped) oscillation, e is the charge of the electron and ν is the frequency of oscillation. The number of photons emitted per second is found by dividing by $h\nu$:

$$A = \frac{16}{3}\frac{\pi^4 \nu^3 e^2 a^2}{hc^3}.$$

Quantum mechanical calculations of the interaction of a one-electron atom with an electromagnetic field, when combined with the probability arguments of Einstein, yield for the probability of spontaneous emission of a photon (per second) corresponding to the electronic jump from n to m,

$$A_{nm} = \frac{64}{3}\frac{\pi^4 \nu^3 e^2}{hc^3}\left|z_{nm}\right|^2.$$

The correspondence of these two equations is visualized by associating the amplitude of oscillation, a, with twice the

matrix element, $2|z_{nm}|$. A very simple argument (19) shows that in the limiting case of a few emitting atoms constituting an "optically thin layer," the intensity of the spectrum line should increase linearly with the number of atoms. We must, in addition, remember that the atoms available to radiate a given line form a small fraction of the whole. As a first approximation to the number available, a Boltzmann distribution is assumed:

$$n_n = n_o g_n e^{-\frac{E_n}{kT}} ,$$

where

n_o is the number of atoms per cubic meter in the ground state,

n_n is the number per cubic meter in the state n (the upper state of the transition),

g_n is the statistical weight of the state n,

E_n is the energy of the upper state referred to the ground state energy of zero, and

T is the temperature of the ensemble.

These considerations give for the intensity of the spectrum line in energy units per second radiated in all directions,

$$I_o = A_{nm} \cdot h\nu \cdot n_o g_n e^{-\frac{E_n}{kT}} .$$

On page 97 of Mitchell and Zemansky (20), is a relation between A_{nm} and the more often tabulated f-value, f_{mn}.

In terms of the emission f-value

$$A_{nm} \propto f_{nm} \nu^2 .$$

And hence

$$I_0 = \kappa \nu^3 g_n f_{nm} e^{-\frac{E_n}{kT}}, \qquad (1)$$

where κ absorbs the constants of no interest. Included in κ is the number of atoms n_0, which we do not evaluate in this experiment; so the f-values with which we deal are relative and not absolute. The term "f-value" will be used to mean these relative emission f-values.

Now, if we knew the temperature of the arc, a measurement of the intensities of emission lines would lead to a determination of the f-values. The temperature can be found by applying the same equation to lines for which f-values are known: the known atomic constant and the measured intensity allow a calculation of the temperature.

Whether such a temperature has physical meaning is often debated; and Crosswhite (21) and Duffendack and La Rue (13) summarize the feeling of many investigators that T may be at best only a very convenient parameter. This feeling is more doubtful in extreme cases, for instance where the pressure is reduced to the extent that the arc becomes a glow discharge.

Difficulties are found to present themselves in such experiments, however. The observed relative intensities of

lines may differ widely from calculated values in cases where f-values are known and allow such a calculation. This misbehavior of emission lines is called, variously, self-absorption and self-reversal. Of course, temperature determinations made with such lines will vary in a corresponding manner; see Harrison (22), Crosswhite (21), and Hemmendinger (12); and also references (23) to (26). Experimentally it is possible to avoid the issue by keeping the concentration of atoms, n, very low, as is pointed out by Smit (5).

These difficulties arise because the atoms emitting a line in the arc do not constitute an "optically thin layer." An extension to this simple theory of emission lines is discussed in the next section.

B. Self-Absorption and Self-Reversal

Cowan and Dieke (17) have carried out an analysis of the phenomena to be expected from a much more general model of the arc than that used in the last section. We summarize the relevant theoretical conclusions of their paper as follows: If one represents the relationship between the measured intensity, I, and the calculated intensity, I_o, for lines whose f-values are known, by means of the graph

$$\log \frac{I}{I_o} = \text{function of } \log I_o , \qquad (2)$$

one finds that the curves obtained for different multiplets

a. approach the horizontal asymptote

$$\log \frac{I}{I_o} = 0$$

for small I_o,

b. drop off (to the right) for large I_o, finally approaching the slope $-\frac{1}{2}$ for resonance lines and the slope -1 for Doppler lines (for moderate values of I_o; for extreme values, the slope in the Doppler line case tends to $-\frac{1}{2}$, in a behavior reminiscent of the absorption curve of growth),

c. drop off more, for a given I_o, as the current increases, and

d. drop off less, for a given I_o, as multiplets with higher excitation initial (upper) states are selected.

Often self-absorption is defined as the saturation of spectrum lines which would occur in a homogeneous source, as the intensity I_ν approaches the blackbody ceiling, $B_\nu(T)$. Self-reversal is associated with the complicated line profiles often seen in the spectrum of an arc, The curves given in the above reference do not allow a distinction between these two effects in an arc. Nevertheless we shall, in working through the data collected in this experiment, keep alert to the possibility of distinguishing between them; for it has been suggested that self-reversal might result in a tendency for the curves of Eq. (2) to approach, for low values of I_o, horizontal asymptotes less than zero for certain multiplets, i.e.,

$$\lim_{I_o \to 0} \log \frac{I}{I_o} = a < 0 \,. \qquad (3)$$

By self-absorption we will mean, as above, the tendency of the plot of Eq. (2) to drop off from its horizontal asymptote, whether that asymptote be 0 (no self-reversal) or otherwise.

A desirable experimental program now becomes clear. We shall measure intensities of as many as possible of the lines for which f-values are known. We will attempt to select those lines not affected by self-reversal or self-absorption and use Eq. (1) to obtain the effective arc temperature. This temperature will enable us to calculate, again by Eq. (1), the unperturbed intensity, I_o, for all the other measured lines. Then we will compare I and I_o, in the manner

described above, for the lines that are affected by self-absorption and self-reversal.

Changes in temperature, self-absorption and self-reversal with temperature, pressure, and location in the arc, will be studied as part of the program.

All these measurements may be done with relative values of intensities and with relative f-values, inasmuch as we have no way of determining absolute values of n_o, I, or I_o in this experiment.

III. APPARATUS AND PROCEDURES

A. Layout of Apparatus

Fig. 1 shows the layout of the apparatus. It is clear that the requirement that the operator be near the arc, to make focusing adjustments, makes it impossible for him to make measurements in the grating room simultaneously. The solution of this problem by automatic operation of the instrument, more fully described in the subsequent pages, allows the operator to stay in the source room near the slit. The tracing produced by the recorder contains the desired information. A glance at the tracing tells one the position of the scanning photocell and of any malfunctioning of the instrument.

B. Mounting of Photocells

In mounting the photocells to scan the spectrum, the most difficult problem faced was one of alignment. Not only must the exit slit stay accurately on the Rowland circle, but a line from the photocathode through the exit slit must strike the grating, which, of course, is not at the center of the circle. This problem was solved by a design employing the theorem of geometry that the angle subtended by a given segment of a circle at the center is twice that subtended by the same arc at a point on the circumference. Thus as the scanning photocell moves over a length of the Rowland circle Δs, the angle subtended by Δs at the grating is $\frac{\Delta s}{2r}$. By an appropriate system of gears it is possible to cause the photocell and exit slit to rotate relative to the line from the center of the circle through an angle $\frac{\Delta s}{2r}$. In this way the line from the photocathode through the slit always points to the center of the grating.

Single letters in the following description refer to Fig. 2. The main portion of the carriage (A) rides along the track which is part of the spectrograph. A shaft which is geared to a rack (B) mounted on one of the spectrograph rails rotates the top assembly (C) so that it points to the grating; and the exit slit is mounted directly over this shaft. There are two such carriages, one a mirror-image of the other so that the two photocells may be placed in close conjunction.

Final focus is obtained by moving the entire slit and photocell mechanism toward or away from the grating by pinion (E). The slit may be adjusted vertically, and the photocell may be adjusted in all three directions relative to the slit.

An optical finding apparatus was designed which does not disturb the exit slit or the photocell. In one end of the slit is milled a square aperture. Behind this hole is a totally reflecting prism (G) which directs the light upward to the eyepiece (H). The face of the prism is slightly larger than the aperture, so that above and below the square, as seen by the eyepiece lens, a small length of slit appears. When used on the spectrum these small lengths serve as illuminated fiducial marks.

Manual slow motion of the photocell carriages is provided by a crank geared to the same rack (B) which causes the rotation of the top plate (C). Mechanical scanning of the spectrum is provided for one of the carriages by mounting a motor (F) so that it can be swivelled into a position where its shaft bears on the crank described above. The force required to propel the carriage down the track is variable to the extent that wire or cord drives proved unsuccessful. It was found that a commutator motor produces so much static as to interfere with the experiment; the motor in use is an induction motor.

C. Choice of Ratio Circuit

The recent development of the photomultiplier tube has opened up vast possibilities for spectrophotometry because of the ease of calibration, and the rapid nature of the measurement even at spectroscopic light levels.

The photomultipliers employed in this experiment were the 931 and the 1P21. The characteristics of these tubes are discussed in reference (27).

Three factors were involved in the choice of circuit. The first was that long-range plans for the instrument anticipated its use with the graphite tube electric furnace. Furnace emission spectra represent a fixed temperature, but the density of atoms decreases gradually with time. The intensity of emission lines then also decreases, but, to a first approximation, the ratio of the intensities of any two will remain constant. It was felt that, even in the case of an arc, isothermal fluctuations might occur in which the line intensity ratio would be constant. Of course the continuous background may not change in just the way the lines do; therefore, the ratio of readings on two emission lines, which include both line and some continuum, will, to a second approximation, not be quite constant. Nevertheless, the advantage seemed to lie in favor of a ratio measuring circuit employing two photocells.

It is of interest to compare the response of a single photocell instrument to small non-isothermal fluctuations

with that of a twin photocell, ratio measuring circuit. From Eq. (1) we write for the intensity of a spectrum line in the absence of self-absorption and self-reversal,

$$I_o = \kappa \nu^3 g_n f_{nm} e^{-\frac{E_n}{kT}}.$$

This quantity is the one measured by the single photocell circuit, and the relative change in this quantity due to a small change of temperature is:

$$\frac{\Delta I_o}{I_o} = \Delta \log I_o = \frac{E_n}{kT^2} \Delta T.$$

We have taken a typical line of upper state E_n and have assumed a basic temperature T. The ratio circuit measures instead:

$$\frac{I_{o1}}{I_{o2}} = \frac{\kappa_1 \nu_1 g_{n_1} f_{n m_1}}{\kappa_2 \nu_2 g_{n_2} f_{n_2 m_2}} e^{-\frac{E_{n_1} - E_{n_2}}{kT}},$$

and the relative change is:

$$\frac{\Delta\left\{\frac{I_{o1}}{I_{o2}}\right\}}{\left\{\frac{I_{o1}}{I_{o2}}\right\}} = \frac{E_{n_1} - E_{n_2}}{kT^2} \Delta T, \qquad (4)$$

for similar typical lines. It is clear that less change is to be expected in the ratio circuit. None should occur for lines from the same upper state except due to changing continuum, self-reversal, or self-absorption.

The second factor in the choice of a circuit was that the current which flows in a photomultiplier even when no light impinges on the photocathode, the so-called "dark

current," must be accounted for. In a simple DC circuit with one photocell it would be necessary to subtract from each reading of low level light intensities the simultaneous value of the dark current. In a DC ratio circuit there would, indeed, be no way at all to correct for dark current, inasmuch as one would have measured the ratio of two signals,

$$v = C\,(I + J)\ ,$$

where I is the intensity of radiation on the photocathode, C describes the response of the instrument to radiation of a given wavelength, and J represents the light level equivalent to the highly erratic dark current. This consideration led us to operate the circuit on AC. The modulation is accomplished by chopping the light beam before it enters the spectrograph. Then the ratio measured is simply one of two AC signals of equal frequency and phase.

The third reason was the desirability of changing the very high impedance of the photomultiplier signal to one of low impedance. Modulation of the signal allows one to use the cathode-follower for this purpose without having to guard against DC drift. The cathode follower is very linear and presents a very high impedance to the input circuit; both of these characteristics are very desirable in this application.

These considerations led us to the design of a twin photomultiplier photometer, a detailed description of which is given in Sect. E.

D. Choice of Method to Record Data

The measurement of the instantaneous ratios of emission line intensities was initially done by connecting a transformer primary from the cathode of the cathode-follower of one photomultiplier ρ' to the slider of the potentiometer which formed the cathode resistor of the other photomultiplier ρ'' (Fig. 3). The secondary of the transformer was connected across the Y axis of an oscilloscope. The oscilloscope then showed the wave form of the difference signal. Now let the photocell ρ'' (feeding the cathode resistor which had the potentiometer slider) be placed on the brighter spectrum line. Then with the slider at the position of maximum resistance to ground, $F = 1.00$, a signal appears on the screen having the same phase as the signal from ρ''. With the slider at some much lower resistance-to-ground position, $F \ll 1$, one sees a signal with the opposite phase, indicating that now the signal between the potentiometer slider and ground is less than the signal across the other ("standard") resistor R_2'. In between these two extreme slider positions there is a point of balance, F_o , when the pattern on the oscilloscope screen reduces to a line.

$$\nu' - F_o \nu'' = 0 . \qquad (5)$$

The ratio of the resistance between slider to ground on the potentiometer to the resistance of the standard resistor provides the ratio of the light intensities if the photocell responses k_λ are known. This ratio may be read off a scale

(previously calibrated for any non-linearity in the resistance wire) on the potentiometer shaft. Compare Huldt (28).

A second step was the provision of a meter which would indicate the proper potentiometer balance by passing through an extreme reading (Fig. 4). This involved replacing the oscilloscope mentioned above with several stages of (tuned) amplification, a triode detector, and a fifty micro-ampere movement meter with a variety of shunts between the detector and a fixed voltage tap. Compare (29).

The instrument described above was used with the 21-foot Rowland spectrograph. In order to use the instrument with the Paschen spectrograph, it became necessary (for reasons discussed in Sect. A) to render the operation of the apparatus and the recording of data automatic, if possible. The manner in which a Brown Recording Potentiometer was incorporated in the circuit to accomplish this third step will be described in the next section. A detailed description of the parts and electrical behavior of the entire instrument will be given in Sect. E and Sect. F.

E. Instrumentation

The following is a description of the electrical parts of the apparatus.

The circuit begins (see circuit diagram, Fig. 5) with two photocell units, each consisting of a photomultiplier mounted on a small metal chassis. This chassis also supports the cathode follower tube associated with the photocell. It also shields various components associated with the photocell and cathode-follower.

These chasses are mounted on carriages on the focal curve of the Paschen spectrograph as described in section B. Cables bring filament, plate, and photocell power from a movable relay rack nearby. These cables also conduct the signal from the cathode-follower tubes via the relay rack to the cathode resistors R_2 which are mounted in the Brown Recorder. The recorder is placed in the source room so that the operator can keep track of the progress of the experiment.

As in the simpler circuits described in the last section, one of the cathode resistors, the standard resistor, R_2', is held fixed (although it is really adjustable for reasons of calibrating the readings), while the other cathode resistor R_2'' is used as a potentiometer. This potentiometer is linked directly to a shaft of the Brown Recorder balancing system by a section of rubber hose 2 inches long.

The primary of the transformer T is connected from the

standard resistor R_2' to the slider of the potentiometer R_2'', and through the condensers C_1. These condensers isolate the DC parts of the circuit from the transformer.

Now the secondary winding of the transformer will give a signal whose amplitude indicates the amount of off-balance between the voltages at the points across which the primary of the transformer is connected, and whose phase indicates the direction of the unbalance. Again, this is the same in the simpler circuits.

At this point it will be necessary to digress briefly to describe the operation of a Brown Recording Potentiometer as it is usually intended to operate. In principle, in the Brown Recorder an unknown DC potential is compared to that of a standard cell using a working battery exactly as in a simple potentiometer. In place of the customary meter on which one seeks a zero reading while adjusting the potentiometer slider, the manufacturers have installed a chopper which converts the DC signal, indicating off-balance, if any, in the potentiometer, to an AC signal. This AC signal is then sent through a transformer to the grid of the first of a series of amplifier tubes. After amplification, the signal is impressed across the detector windings of a two phase induction motor. This motor is connected mechanically to the potentiometer slider. The action of the transformer and of the two phase motor is such that the slider is always driven toward the position it should occupy to reduce the

off-balance signal to zero. The motor at the same time moves the indicating pen, which traces a record of the slider position in terms of per cent of total slide wire resistance value, F. Schematically the mechanism is represented as in the Fig. 6, taken in part from the Brown Company publication (30).

It might seem that in order to use the features described above in the spectrophotometer, it would be necessary to convert the signal to DC (in a phase sensitive way, e.g., by the use of a phase sensitive detector), and also to rewire the components of the Brown Recorder so that the slide wire already present would serve the function of the potentiometer previously used as cathode-follower resistor, R_2''.

A much simpler scheme somewhat similar to that of Crosswhite's (21) has been adopted which avoids any conversion of the signal. The AC signal is fed directly from the transformer secondary to the grid of the first tube in the Brown Recorder amplifier, by-passing all the DC components and the chopper provided for DC measurements. The signal then activates the motor to drive the slider R_2'' and the pen to the position of balance.

A switch S_2 is provided which allows the measurement or inspection with an oscilloscope of the signal given by each photocell unit. This switch cuts out the transformer, which otherwise would allow no comparison of the voltages of the two signals.

The power supplies, switches, meters, and cable connections are all mounted on the relay rack.

A very grave danger in the construction of such a circuit to operate at 60 CPS is that the signal may be confused by the pickup of electromagnetic "hum." The following precautions were taken to minimize this hum:

1. All "ground loops" (wide separation of return paths) and superfluous grounds were eliminated. Cables were twisted.
2. Components associated with the high impedance signal from the photocells were shielded.
3. All large iron masses, such as panels, were removed.
4. A very well shielded transformer was used. The manufacturer's figure was -75 db.
5. Care was taken in connecting AC plugs with the appropriate side on the hot wire, especially for the Brown Recorder.
6. Identical parts were installed for symmetrical elements of the ratio circuit.
7. Filament power was provided by a 6-volt auto battery.
8. No ripple can be permitted in the signal of the source, therefore, the tungsten lamp used for wavelength standardization, as well as the arc itself, were operated from a 110-volt DC generator, with appropriate ballast resistors.

F. Analysis of Circuit

The analysis of electrical properties of the circuit is analogous to that for a Wheatstone bridge circuit (31).

By the use of Thevenin's theorem and of simple equivalent circuits for the tubes, we can reduce the circuit to the input side of the transformer to a black box containing a perfect voltage generator with a series resistance. The respective values of these components are

$$V = \frac{R_2 \mu}{R_2(1+\mu)+r_p}\left\{v' - Fv''\right\} \tag{6}$$

and

$$R = \frac{1}{R_2(1+\mu)+r_p}\left\{R_2 r_p(1+F)+(1+\mu)(1-F)FR_2^2\right\},$$

where

R_2 is the value of R_2' and R_2'',

r_p is the plate resistance of the 6AK6 cathode-follower tube,

μ is the amplification factor of the cathode-follower tube,

F is the fraction of R_2'' between the slider and ground,

v' is the peak-to-peak voltage of the signal across R_2', and

v'' is the peak-to-peak voltage of the signal across R_2''.

The first of these equations restates the fundamental principle of the ratio circuit--that the error signal has a magnitude increasing with the amount of off-balance and a phase indicating the direction of off-balance. The second equation implies that the impedance of the network feeding the transformer changes as F changes.

The transformer T is now connected to the terminals of the black box. The input impedance of the first tube in the amplifier, to which the secondary winding of the transformer is connected, is high. Therefore the effect on the black box is the same as if one were to connect across its terminals an inductance, L (the magnetization inductance of the transformer), and a resistance, P (the DC resistance of the primary winding). If the resulting equation,

$$V = \{R+P+j\omega L\} i \ ,$$

is solved for i, two important pieces of information are found. The phase of i, and therefore of the signal received by the amplifier tube, varies over a range of about 20° as F varies from 0 to 1.00. This variation of phase is too small to result in serious loss of sensitivity due to the phase sensitive characteristics of the recorder. A measure of the precision of the circuit is obtained by calculating how much F must vary from F_o in order to produce a given amplitude of error signal. This calculation shows that the absolute

precision is greatest at the low end of the scale, and the relative precision is greatest at the high end.

G. Testing of Instrumentation

One of the requirements for operation of the ratio measuring circuit is that the output of each component of the circuit connected to the input winding of the transformer be strictly linear with respect to changes of light intensity at each photocell. Some of the means used to test for linearity are now described:

1. Measurements of the DC current produced by the photocells under various degrees of illumination were made, by inserting a micro-ammeter in series with the plate resistor of the photocell (R_6 in Fig. 5). It was found that the most intense spectroscopic illumination would not produce saturation of the photocell current.
2. The linearity of the cathode followers was tested by measuring the AC signal across the cathode resistor, for each of a number of AC voltages impressed on the grid. Linearity was found to hold even with signals far larger than any encountered in practice, which are at most 2 volts peak-to-peak.
3. With the instrument in operation, the signal given by either photocell unit was exhibited on the oscilloscope screen. As known fractions of the light were cut out by Kodak neutral density filters, the amplitude of the signal was measured and found

to be linear for both photocell units.

4. With the instrument in operation, the ratio reading being given by the recorder, known fractions of the light incident on the photocell p'' having the larger signal v'' were cut off. This signal v'' then decreased until it was equal to v', while the reading, F_o, on the recorder chart increased to 1.00. Then on reversing switch S_1, the signal on photocell p'' could be reduced even more, and the recorder would indicate smaller and smaller ratios F_{ro}. The ratios F_o, together with the reciprocals of the ratios F_{ro}, formed a sequence of readings which, when plotted against the relative amount of light impinging on photocell p'', gave a confirmation of linearity.

5. Finally, with the instrument in operation, the signals given by the two photocell units were adjusted to be equal and very large (about 5 volts). The recorder was then cut in and it gave a reading of about 1.00. Then Kodak neutral density filters were placed in front of the exit slit of the photocell p' which feeds the standard resistor, and the ratios, F_o, were recorded. This procedure was repeated with different initial signals. The operation of the instrument at any time was represented by a point in a coordinate system with axes $\log v'$

and $\log r''$ (or, on the basis of tests 1 to 3, with axes $\log I'$ and $\log I''$); by each point was entered the corresponding recorder reading, F_o ; and all the points with a given F_o were found to lie on a 45° line,

$$\log I' = \log I'' + \log F_o.$$

On the basis of these tests, it was concluded that the instrument was free from electrical sources of non-linearity.

Scattered light in the spectrograph room was reduced by observing the following precautions:

1. The front surfaces of the photocell carriages were masked with black cardboard to prevent multiple reflections from the grating. These masks appear in Fig. 2.
2. The cathode follower tubes were painted black.
3. The grating case was painted flat black.
4. Regions on the grating which scatter large amounts of light were masked.
5. Each photocell was painted, leaving only a small window.

Scattered light will have its maximum effect when one deals with low light intensities compared with large light intensities. One extreme case for which a measure of the scattered light can be obtained, is when the photocell p' is set in the

violet part of the calibration lamp spectrum. Most of the scattered light then received by p' is of longer wavelength than the spectrum wavelength λ' on which it is set. Therefore, if a filter which cuts off all wavelengths shorter than Λ, where $\Lambda > \lambda'$, is introduced before the exit slit of the photocell, the scattered light will pass through unaffected while the direct spectrum wavelength λ' will be cut out.

This test was carried out using a filter which cut out all wavelengths shorter than $\Lambda = 4000A.$ It was found that with photocell p' at 3800 A, the scattered light added 5 per cent to the signal produced by the direct spectrum. We conclude that scattered light did not disturb the experiment.

The photocell units are provided with trimmer condensers C_2 which allow precise adjustment of the phase of the signals to equality. With the two signals in quadrature on the oscilloscope, one adjusts these condensers (the shaft protrudes from the shielded photocell unit chassis) until a straight line results. It was found that unless this was done, no clear-cut balance marked the proper slider setting, F_0, for the potentiometer R_2''; and once it was done, the signals v' and v'' appeared to stay in phase with each other for any value of the signal magnitudes.

One unexplained misbehavior of the instrument must be mentioned in this connection. This effect was observed in varying degrees over an interval during which three spectrographs were used and during which each component of the circuit was altered at least twice. The effect observed was

that, with the instrument operating, a change in the amount of light from the source changed the recorder reading slightly, whereas the reading should remain unchanged if the light is cut out uniformly with respect to wavelength and uniformly over the dimensions of the slit, e.g., if a neutral density filter is used. Some of the possible causes of this phenomenon are now considered.

1. Numerous tests for linearity of the instrument were described at the beginning of this section which eliminate the possibility that electrical nonlinearity is the cause of this effect.
2. Precautions taken against electromagnetic hum pickup were described in Sect. E. Tests for the success of these precautions consisted of moving various components of the circuit about, and of holding a source of strong 60 CPS magnetic field (a soldering gun) close to the components. The ambient hum level was in this way shown to have negligible effect on the circuit.
3. It was mentioned in the immediately preceding paragraph that the signals v' and v'' stay in phase with each other, as shown by the passage of the error signal to a precise straight line when the slider of R_2'' is adjusted to balance. The calculations described in Sect. F. showed that the phase of the

difference (error) signal varies, but has no effect on the operation of the instrument.

In addition, measurements of the magnitude of the phenomenon were taken and applied to the data in the form of corrections; it was found that these corrections produced no significant changes in the data. On the basis of all these facts, it was decided to discount entirely the possibility that this phenomenon affects the data obtained from the apparatus.

H. The Iron Arc

Considerable attention was devoted to stabilization of the iron arc. Assorted shapes and sizes of electrodes and different kinds of wind shields were tried to no avail. A rather novel variation was the application of a magnetic field along the axis of the arc by placing a strong bar magnet on the end of the top iron electrode. The magnetic field should, in principle, keep at least the electrons more confined than otherwise. The actual result is that the arc, which normally flickers within some envelope of positions, flickers so much faster that it appears to fill the envelope completely.

Electrical stabilization, by the introduction of series inductance and/or parallel capacitance, and by the construction of a circuit like that used by Potter and Scott (32), was not effective against the slow and erratic type of change in position encountered in the arcs used.

The presence of a small spherical bead on the lower electrode is imperative; and it was a combination of such a bead, wind shielding, and low current which finally produced an arc needing only occasional slight translations to keep its image on the slit.

Effective wind shielding was obtained by operating the arc in a vacuum arc chamber. This chamber, in Fig. 7, has a vacuum connection and seal, is water cooled, has two removable quartz windows, and provides for adjustment of the upper

electrode by a sylphon bellows.

As the pressure in the arc chamber and the current in the arc are varied, the arc goes through various modes of flickering and envelops itself more or less in a yellowish cloud of iron oxide. For a given pressure there is generally a current at which this arc will run very quietly; there is another, lower, current at which the surrounding cloud appears to vanish, leaving only a faint blue core, (which tends, again, to flicker badly). Very approximate values of these parameters are given in the following table:

Pressure in Cm of Hg	Approximate Value of Highest Current in Amps	
	Stable Operation	No Envelope
4	10	3
40	5	3
76	3	

There is a tendency for the windows of the arc chamber to become cloudy more rapidly as one increases current or pressure. This can be lessened by allowing a very slight leak to blow air across the window.

I. Arrangement of Apparatus at Slit

The source is mounted on a platform which can be adjusted in the vertical and lateral directions, by screw adjustments, to keep the image of the source on the slit. See Fig. 7, (A). A lens (B) of 18 cm focal length focuses an image of the source on the slit, magnified 4 times.

The light beam is modulated to produce the 60 CPS signal for the circuit by a synchronous motor turning a chopper (C) through the beam between the lens and the slit. In order to adjust the phase of the error signal given by the circuit and amplified by the Brown amplifier so that it has the proper 90° relation to the power windings of the two phase motor, the chopper motor can be rotated as a whole about an axis along its shaft.

A very simple and effective vacuum system was arranged using Cenco Hyvac pump, an open end manometer, and a stop-cock for introducing an artificial leak. A dust trap was provided which prevented copious amounts of iron arc debris from entering the pump.

J. Operating Procedures

In order to measure the relative intensities of emission lines at different wavelengths, the distribution of light by the spectrograph and the response of the photocathode of the photomultiplier as a function of wavelength must be taken into account. (See also App. I.)

This calibration is done with a tungsten ribbon-filament lamp; a record is made of the spectrum of the lamp with all slit settings the same as when the iron spectrum is traced. The type of lamp used was a G.E. microscope illuminator with a rated current of 18 amperes. The lamp was run at 14 amperes which gave a temperature in the neighborhood of 2200° Kelvin. The lamp temperature was measured with an optical pyrometer. The wavelength scale for the iron spectrum is established by recognition of prominent lines. In order to provide the operator with a wavelength scale for the lamp spectrum, microswitches were mounted on the spectrograph rail and connected to indicator lights in the source room. The wavelength calibration is now done by substituting portions of the lamp spectrum for those regions of the spectrum of the arc in which no iron lines of interest appear. The image of the lamp filament is focused on the slit by the same lens used for the arc by placing the mirror (D) in the position shown in Fig. 7. See also Fig. 1. The tracing obtained displays the spectrum of iron interrupted by occasional sections of the

continuous spectrum of the lamp. The measurements of temperature made with the pyrometer are corrected for the imperfect reflection of the mirror.

The tungsten lamp spectrum can be used for calibration because its distribution of radiant energy is known. The energy emitted at any wavelength is about half that of a blackbody with the same color temperature; the exact fraction has been tabulated (33). Then

$$I_{\lambda t} = \epsilon(\lambda) B_\lambda(T) ,$$

where

$I_{\lambda t}$ is the intensity of the lamp per wavelength interval,

$B_\lambda(T)$ is the value of I_λ for a blackbody of temperature T,

$\epsilon(\lambda)$ is the tabulated emissivity.

If we define the photocell response in terms of the "photocell response constant" k_λ (in units of intensity per unit wavelength per volt signal across R_2), then

$$I_\lambda = k_\lambda v . \tag{7}$$

The tracing of the lamp spectrum provides the relation which allows evaluation of k_λ:

$$I_{\lambda t} = \epsilon(\lambda) B_\lambda(T) = k_\lambda v_t . \tag{8}$$

These relations will be used in Sect. K.

The principle of the calibration run has now been pointed

out. The actual procedure of taking the iron arc and lamp spectra will now be described.

First, the ratio reading of the Brown Recorder does not correspond exactly with the fraction, F_o, of the potentiometer slide wire needed for the balance condition. Calibration of the chart reading,

$$F_o = \text{function of reading}, \qquad (9)$$

is made with a Wheatstone bridge.

Second, the iron spectrum is inspected to identify the lines whose relative f-values have been tabulated, and which, therefore, will provide the desired information about temperature, self-absorption, and self-reversal. The lines whose f-values have been given by Carter (16) are confined to the regions between 4200 A and 4600 A and between 5100 A and 5500 A. Numerous low level lines measured by King (4) lie in and near these regions. It is in these regions of the spectrum, then, that measurements are to be taken.

Third, the lines in these regions whose f-values are known present an enormous range of intensities. The instrument is capable of giving readings differing by a factor of 50; one must then select the scale so that the greatest number of useful lines will have intensities in such a range. (It is anticipated that future use of the switch S_1 will increase this factor to 2500.) The lines selected for

measurement must represent multiplets with a wide range of upper excitation potentials, in order to enable a good fit of T in Eq. 1. In order to investigate the effects of self-absorption and self-reversal, the multiplets observed should contain several arc lines of known f-value, and these lines should cover a large range of intensities. These are the factors to be considered in selecting the lines whose intensities will fall within the range of operation of the instrument. As a rule, an effort was made to set the scale in each scanning of the spectrum so that the strongest known line of multiplet 41 (4383 A) gives a reading of almost 1.00, for the ratio F_o.

Fourth, the following considerations enter into the setting of the scale of the instrument so that it will measure lines which fulfil the requirements just laid down:

1. The line at which the standard cell ρ'' is placed can be selected to aid in choosing the scale of the instrument. All lines within a multiplet will retain their relative intensities unchanged for most of the fluctuations in an arc, and it would seem desirable to relocate the standard photocell ρ'', each time a different multiplet was under consideration, to a line of the same multiplet. However, the advantage of automatic scanning and the need to study lines from several multiplets make it desirable to

leave ρ'' fixed on one line in spite of this effect, which was shown by Eq. 4 to be small. Hence, requirements for the standard line are only that it be strong (Eq. 5), that it be not perturbed by self-absorption or self-reversal; and that it be away from the region to be scanned by photocell ρ'. There is evidence that lines from multiplets 152 and higher can be used as standard lines.

2. The measurements of line intensities are greatly simplified by widening all lines artificially until they assume a flat-topped shape, for then the altitude of the profile would suffice as a measure of the relative intensities. This end is achieved by widening the entrance slit of the spectrograph, or the exit slit of the scanning photocell. It was chosen to widen the spectrograph slit. The exit slit of the scanning photocell ρ' must be kept small to conserve resolution and the exit slit of the standard photocell ρ'' must not exceed the width of the line on which it was set (else the very variable continuum introduce bad fluctuations); but within these limits, both slits can be altered to select the desired intensity range of lines which shall give useable ratios on the recorder.

3. The selection of scale may be remade for convenience when a separate calibration run is made by changing

the exit slit settings; if a simultaneous calibration run is made, still one other available parameter becomes useful: the variation of the response of the entire instrument by a filter. Thus by placing a Corning signal blue filter before the slit of the spectrograph, the relatively poor emission of the tungsten lamp in the blue may be effectively made greater without at the same time seriously weakening the green part of the iron spectrum. Typical slit settings for a run with separate calibration follow:

	Slit Settings for Operation with	
Slit	Arc Spectrum	Lamp Spectrum
Entrance slit		
Length	3.0mm	3.0mm
Width	0.38mm	1.50mm
Scanning slit		
Region	First order	
(Approx. width of spect. lines)	0.4mm; 0.7A	
Slit width	0.05mm; 0.17A	0.05mm; 0.17A
Standard slit		
Wavelength	4260A, Second order	
(Approx. width of spect. lines)	0.4mm; 0.7A	
Slit width	0.3mm; 0.51A	0.30mm; 0.51A

Fifth, the scanning photocell must be driven at such a rate that the recorder (which has a 2-second pen sweep) will have time to follow the violent changes of ratio encountered in scanning a spectrum. The appropriate speed was found to be about 5 mm per minute. Inasmuch as the dispersion of the spectrograph in the first order spectrum is about 3.4 A per mm, this driving speed corresponds to 17 A per minute. The chart speed of the recorder is usually set at its top speed of .8 inches per minute. Thus the final tracing has a dispersion of 14 A per inch.

These five steps need not be taken each time a new run is contemplated. The next two steps, however, pertain to the time of the actual run.

Sixth, the instrument is turned on and photocell ρ' is set at one end of the spectrum. From the source room, the operator sets the scanning photocell drive motor into operation and monitors the arc as the tracing is made. The photocell carriage is moved manually between one spectral region and the other. There are some circumstances when difficulty is encountered in taking data due to the part of the arc from which light is admitted by the slit to the spectrograph. In general, it was very difficult to get good records of spectra from the edge of the arc. The sluggish action of the recorder in this instance seems to be related to the excessive amount of noise observable when the signal

is displayed on the oscilloscope. Often the recording made of the intensity variation over a line, instead of being flat on the top, is more or less skewed, indicating that the various parts of the line, being due to the light entering various parts of the slit, actually present differing intensities. This is because the arc is being cut by the non-negligible field of view of the apparatus; and in the case of a run being taken over the spectrum from the edge of the arc, there is a progressive change of arc conditions being represented by different parts of the line as it is focused at the Rowland circle. It appears that the actual change of conditions is not so much one of temperature but of the amount of continuum present.

Seventh, during the progress of the run, the arc current and the pressure in the vacuum system must be watched closely, since specific operating conditions are desired. Small changes in the current are most easily corrected by very slight changes in the arc electrode separations; the pressure is regulated with the stopcock which allows air into the vacuum system. As the tip of the upper electrode burns away, the electrode must be lowered to keep the arc column length constant. This adjustment, as well as the more slight one just referred to, is made with the arrangement labeled (J) in Fig. 7. Finally, the lamp temperature is measured with the optical pyrometer.

This concludes the discussion of experimental procedure.

K. Reduction of Data

From each run of the spectrophotometer, a tracing is obtained on which appear the lines of the spectrum of the iron arc and the continuous spectrum of the calibration lamp. The method by which the data on relative intensities of lines in the iron spectrum were obtained from these records will now be described.

The quantity F_o is needed in the calculations; but F_o is not exactly the same as the quantity given by the deflection of the recorder pen. The calibration of F_o in terms of the readings obtained from the recorder chart was described on P. 37. The raw, uncorrected readings corresponding to F_o are designated C_o. When the slider of the potentiometer R_2'' is adjusted by the recorder so that the error signal is zero, then the fraction, F_o, of the resistance R_2'', which is between the slider and ground, gives the ratio of the signals v' and v'', which appear across R_2' and R_2'', respectively. That is, using Eq. (5),

$$F_o = \frac{F_o R_2''}{R_2'} = \frac{v'}{v''} \quad . \tag{5'}$$

The use of a wide entrance slit gave broad flat-topped line profiles on the tracing. The relative intensities of the lines are, therefore, proportional to the heights of the profiles on the tracing. Then

$$I_{\lambda'} = k_{\lambda}' v'$$

and

$$I_{\lambda''} = k_{\lambda}'' v'' \quad , \tag{7'}$$

where

I_λ is the relative intensity of the line at wavelength λ on which photocell p is set,

v is the magnitude of the voltage appearing across R_2, and

k_λ is the photocell response constant, in units of intensity per volt signal.

(Peak-to-peak values of the square waveforms are always used.)

Combining Eq. (5') with Eq. (7') we have for the ratio of the intensities of two iron spectrum lines,

$$\frac{I_{\lambda'}}{I_{\lambda''}} = \frac{k_{\lambda'} v'}{k_{\lambda''} v''} = \frac{k_{\lambda'}}{k_{\lambda''}} F_o \quad .$$

If the spectrum of the iron arc is now replaced by the spectrum of the ribbon filament lamp, the photocells remaining at wavelengths λ' and λ'', the ratio measured will be, using Eq. (8),

$$\frac{I_{\lambda' t}}{I_{\lambda'' t}} = \frac{k_{\lambda'}}{k_{\lambda''}} F_{ot} = \frac{\epsilon(\lambda') B_{\lambda'}(T)}{\epsilon(\lambda'') B_{\lambda''}(T)} \quad .$$

Combining this equation with the one above, we have for the ratio of the intensities of two iron lines:

$$\frac{I_{\lambda'}}{I_{\lambda''}} = \frac{\epsilon(\lambda') B_{\lambda'}(T)}{\epsilon(\lambda'') B_{\lambda''}(T)} \frac{F_o}{F_{ot}} \quad .$$

If the photocell p'' remains fixed at λ'',

$$\frac{I_{\lambda''}}{\epsilon(\lambda'')B_{\lambda''}(T)}$$

is constant. Hence the relative intensities of lines recorded by the moving photocell will be

$$I = \frac{\epsilon(\lambda')B_{\lambda'}(T)}{F_{ot}} F_o \equiv k_\lambda F_o . \qquad (10)$$

Graphs of $\epsilon(\lambda)$ and $B_\lambda(T)$ over the wavelength region covered by the observations were prepared from data given by Forsythe and Worthing (33) and by the International Critical Tables, respectively.

The specific procedures followed in the reduction of data are now enumerated. Three significant figures were retained throughout.

1. The chart reading for each spectrum line is obtained from the position of the best horizontal line across the top of the tracing of the line. Often two lines which appear blended give a tracing on which it is possible to distinguish the altitudes of the figures which would have occurred had the lines been separate (See drawing).

A triple combination of profiles is found for three lines including 5216 A; a still more complicated case occurs between 4216 and 4227 A. Now the altitudes of the figures found on the chart, $C_o(line)$, are converted into values of

$F_o(line)$ by Eq. (9).

2. The best straight line through the continuum near each line is drawn; the value of $C_o(cont.)$ is converted to the corresponding value of $F_o(cont.)$.

3. A subtraction gives F_o .

The next two operations form a group by themselves:

4. For the wavelength at which each line appears, obtain C_{ot} from the tracing of the lamp spectrum; convert to F_{ot} .

5. Using previously graphed values of $\epsilon(\lambda)$ and $B_\lambda(T)$, form k_λ , defined in Eq. (10).

In many cases two or three runs were taken with a given condition for arc operation; runs with different scale factors (slit settings) can extend the range of intensities of lines which can be measured. The way in which different runs are tied together is now considered. If the two runs were made without any changes having been made in the scale factors, we may average F_o :

6. Plot F_o for one run against F_o for the other, and draw the best radial line through the points. This line established the factor between the two sets of F_o values. Multiplication of the lesser set by this number adjusts the scale so that we may average F_o .

7. Multiply k_λ and F_o , as in Eq. (10), and take logs.

If the second run was made after an interval in which some

change had been made in the apparatus, either for repair or for testing purposes, then the values of k_λ will differ, as well as those of F_o . In this case, the last two steps are interchanged.

6'. Compute $\log I$ values for each of the two runs.

7'. Plot $\log I$ for one run against $\log I$ for the other and draw the best line of unit slope through the points. The intercept of this line establishes the scale factor between the two sets of data. Addition of the scale factor to the lesser set of $\log I$ values adjusts the scale so that we may average $\log I$.

The reduction of the data terminates with these properly averaged values of $\log I$, which are presented for the standard arc in Table IB. The first column gives the multiplet numbers of the lines measured (see P. 49); in the second column are listed the measured lines in each multiplet according to wavelength. The next two columns give the instrument reading for the lamp spectrum F_{ot} and the averaged value of $\log I$ for the standard arc.

IV. RESULTS

A. Temperature of the Standard Arc

The relative intensities of lines emitted by the arc, for which f-values are known and which are not self-absorbed or self-reversed, are related to the temperature of the arc by Eq. (1). This temperature could be evaluated by substituting for each I_o the corresponding value of I (see Eq. (10)), provided lines were used which were not weakened. If more lines were used, the averaged value of T would be more precise. Since there is no a priori way of selecting unweakened lines it is desirable to select T graphically. Eq. (1) is rewritten

$$\log I_o = \log \kappa' + \log \frac{g_n f_{nm}}{\lambda^3} - \frac{e\mathcal{E}_n}{2.303 kT} , \qquad (1')$$

where $\mathcal{E}_n$ is the energy of the upper state of the transition, now expressed in electron volts.* Now replacing I_o by I and rearranging terms, Eq. (1') becomes

$$\log \frac{I\lambda^3}{g_n f_{nm}} = -\frac{e\mathcal{E}_n}{2.303 kT} + \log \kappa' .$$

The data are now plotted in the form

$$\log \frac{I\lambda^3}{g_n f_{nm}} = \text{function of } \mathcal{E}_n . \qquad (11)$$

---

*In all computations, $\log \lambda^3 - 10.8$ was used instead of $\log \lambda^3$. The difference was included in $\log \kappa'$.

Then the best straight line through the points has a slope m related to the temperature by

$$T = -\frac{e}{2.303k}\frac{1}{m} \quad . \tag{12}$$

In preparing to use the $\log I$ data gathered in the experiment, in the graph represented by Eq. (11), a table of

$$\log\frac{\lambda^3}{g_n f_m} = 3\log\lambda - \log g_n f_{nm}$$

was prepared. The values of $g_n f_{nm}$ were taken directly from the tables of King and King (4) and Carter (16). Values of $\mathcal{E}_n$ were taken from A Multiplet Table of Astrophysical Interest, Revised Edition, by Charlotte E. Moore. Lines in the spectra of an element are arranged in this table by multiplets, and the multiplets are arranged and numbered in order of (a) increasing lower state energy and (b) upper state energy. Thus, multiplets 1 and 2 terminate on the ground state, multiplet 15 terminates at 1 volt, etc. $\log\frac{\lambda^3}{g_n f_{nm}}$ and $\log I$ are now added and the sum is plotted against $\mathcal{E}_n$. This graph is shown as Fig. 8. The points plotted were taken in three runs over the spectrum of the so-called "standard arc," which is the center of an arc operated at a pressure of 1 atmosphere and a current of 2.3 amperes DC, using as electrodes $\frac{1}{4}$-inch iron rods. The $\frac{1}{4}$-inch rods were chosen as a compromise between larger rods which allowed the arc to flicker badly, and smaller rods, which burned rapidly. The electrodes are

kept approximately 4 mm apart, and the lens forms a vertical inverted image about 16 mm high and 16 mm wide on the slit. Of this image a rectangle 3 mm high and 0.75 mm wide is admitted by the slit.

It is immediately evident that the points scatter appreciably and do not fit a straight line. Assuming that the condition of thermal equilibrium exists in the arc, this scatter of points is presumably due to conditions in the experiment or in the experiments where the gf-values were measured. If the particular line represented by a point on Fig. 8 is self-absorbed in the arc, the point will lie below the position it would have had otherwise. If the multiplet in which this line occurs is self-reversed, the point will lie lower than it would be otherwise. If in the experiment of Carter a line were self-absorbed or self-reversed, the gf-value would have been too small, and hence the point on Fig. 8 would be raised; since the sources used in the two experiments were different, these effects would not cancel the previous ones. The gf-values of King, being taken from absorption spectra, would be free from weakening effects.

In drawing the straight line through the points in Fig. 8 the following considerations enter:

1. The very strong lines within a multiplet will suffer

more from self-absorption than will the weak lines. Therefore, in the cases where a multiplet contained several measured lines (a few typical multiplets containing several lines are identified on Fig. 8), the lines with high gf-values will be most lowered below the position they would occupy were they to fall on the line whose slope will give the temperature. Consequently, the points representing weak lines have been (qualitatively) weighted more than those representing strong lines.

2. The multiplets which terminate on a low-excitation lower term will suffer more from self-reversal than multiplets whose lower term is high in energy. Hence, the points representing transitions to low-lying states are weighted less heavily than the points representing transitions to high-energy states.

3. Some points lie far off the main group of points for neither of the above two reasons; and therefore, apparently the measurements of gf-values for these lines are incorrect. The most conspicuous of these are some two or three points which are off by a factor of roughly 10.

4. In early stages of the experiment it had been the practice to scan only a small region of the spectrum at one time. It was found that the temperatures determined for each of three main spectral

regions differed from each other considerably. Typical values were as follows: $\lambda\lambda$ 4200-4300, 5200°K; $\lambda\lambda$ 4300-4600, 3900°K; and $\lambda\lambda$ 5000-5500, 4900°K. Later runs were made over all of these regions each time. On Fig. 8 lines are indicated with symbols which show in which of these regions of the spectrum each appears. It can be seen that lines from different regions suggest different temperatures. The possibility that this effect is due to some systematic error in the experiment was investigated in a manner which will be discussed in the next paragraph.

These four considerations led to the drawing of the line seen in Fig. 8, which corresponds to a temperature of 4100°K.

A digression is now made to consider the possibility of systematic error with respect to wavelength in the experimental data. The values of I given by Crosswhite for a similar arc were converted into $\log I$ and compared with the $\log I$'s measured in this experiment. (More specifically, the arc used by Crosswhite was operated at a pressure of 1 atmosphere and a current of 2.2 amperes DC, using as electrodes 3/16-inch electrolytic iron rods. The electrodes were kept 2 mm apart and a mirror formed an image 6 mm high on the slit. A narrow area of the image 1 mm high was admitted by the slit.) First, graphical comparison of $\log I$ values was made using data from one wavelength region at a time; in this way it was found that the temperature of the arc used by Crosswhite

was higher than that of the arc described above by some 300°K. Next, a graphical comparison of all data was made which revealed, in addition, a systematic wavelength discrepancy. This discrepancy is such that Crosswhite's green lines are too faint, relative to his blue lines, by a factor of 1.8, on the basis of the present experiment. This second comparison is not affected by the result of the first, because lines of all excitations were used in both the green and the blue regions of the spectrum.

The gf-values given by King and Carter allow a second, independent comparison of experimental results. These gf-values, and an arc temperature of 4100°K, are used to evaluate for each line the quantity $\log I_o$ given by Eq. (1'). These values of $\log I_o$ are, then, predicted emission line intensities for a source in thermal equilibrium at a temperature of 4100°K, and free from the effects of self-absorption and self-reversal. Now it will be noted that Fig. 8 can be considered as a comparison of these values of $\log I_o$ with the values of $\log I$ obtained in the present experiment; if for each line $\log I_o$ were used to compute $\log \frac{I_o \lambda^3}{g_n f_{nm}}$, and if these were in turn plotted on Fig. 8, the points would fall precisely on the straight line drawn in the figure. Consequently, the difference between the ordinate of any point in the figure and the ordinate of the straight line at the same value of $\mathcal{E}_n$ is the ratio of relative intensities as determined in the two experiments. When Fig. 8 is examined in this way

there is seen a tendency for measured points representing green lines to be higher than those representing blue lines. The magnitude of the difference is such that the green lines are a factor of about 2 times too strong, relative to the blue lines, on the basis of the data of King and Carter. This wavelength discrepancy is equivalent to that found in the comparison of the same data with those of Crosswhite. It is, therefore, likely that the discrepancies represent an error in the experiment arising from some phase of the experimental procedure.

Crosswhite gives a sample calculation (P. 134) exhibiting the various quantities entering into two values of $\log I$ for lines at different wavelengths. Comparison of this calculation with those described above in the section on "Reduction of Data" was made. Two items came to light:

1. The values of $\epsilon(\lambda)B_{\lambda}(T)$ used in the two experiments agree.
2. The readings given by the recording instrument for the run over the lamp spectrum, F_{ot} , in the two experiments, do not agree. The disagreement is such that Crosswhite's lamp readings are too faint in the green, relative to the readings in the blue, by a factor of 1.4, on the basis of the present experiment. This means that the wavelength discrepancy being discussed is <u>not</u> due solely to experimental differences in calibrating procedure.

Any details in which the calibration run and the iron arc run differed were considered as possible causes of systematic error. Investigations of these differences form the subject of App. I.

It appears that the interpretation of the discrepancy considered in the foregoing digression does not enter vitally into drawing of the line in Fig. 8. If lines from the entire blue region are considered as one group and lines from the green as another group, and if a temperature-line is drawn for each group, the two lines obtained are parallel. Consequently the wavelength-dependent discrepancy was ignored as a factor in drawing the line in Fig. 8.

The comments of this entire section are now summarized. The data are plotted as in Eq. (11); in choosing the best fitting straight line whose slope defines the temperature by Eq. (12), the following factors have been allowed for:

1. Self-absorption
2. Self-reversal
3. Some two or three obviously incorrect gf-values.

The presence of an error which is a function of wavelength is considered likely; but this effect is of such a nature that it could be ignored in ruling the line in Fig. 8. The quantities $\log \frac{I\lambda^3}{g_n f_{nm}}$ for the standard arc appear in Table IB.

B. Self-absorption in the Standard Arc

Eq. (2) is used to show the magnitude of the self-absorption effects in the spectrum of the standard arc (defined on P. 49). The quantity $\log I_o$ is computed according to Eq. (1'), with $\log \kappa'$ equal to zero. The quantity $\log \frac{I}{I_o}$ is read off of Fig. 8:

$$\log \frac{I}{I_o} = \log \frac{I\lambda^3}{g_o f_{nm}} - \log \frac{I_o \lambda^3}{g_n f_{nm}}. \qquad (2')$$

The curves obtained for several typical multiplets in the iron spectrum are shown in Fig. 9. The solid portions of the curves were drawn in to fit the points. The conclusions forthcoming from these curves and others not shown (which are other horizontal lines) are these:

1. The graph of $\log \frac{I}{I_o}$ for a given multiplet approaches a horizontal asymptote for weak lines (small I_o), as predicted by Cowan and Dieke (See P. 8.). However, the horizontal asymptote differs for different multiplets (Compare Eq. (3).). These differences will be discussed in Sect. C.
2. The graph of $\log \frac{I}{I_o}$ falls off to the right for larger I_o. The experimental data do not allow an unambiguous determination of the limiting slope of the curves, the significance of which was given on P. 8.
3. The curves drop off less, (from their horizontal asymptote for weak lines, a) for a given I_o, as

multiplets with higher energy initial (upper) term are selected, and again this behavior is as predicted. The amount of self-absorption becomes too small to be detected for lines whose lower terms have excitation potentials above 2.1 volts (a^5P).

C. Self-reversal and Associated Effects in the Standard Arc

The horizontal asymptotes to which the curves in Fig. 9 tend, as I_0 decreases, (a in Eq. (3)) are in Fig. 10A plotted against the excitation potential of the lower term of the multiplet. In Fig. 9, horizontal dotted lines extrapolate some of the curves for very weak lines. The intersections of these lines with the vertical axis (a in Eq. (3)) are plotted against the lower term energy of the multiplet in Fig. 10A.

As has been pointed out in Sect. A, there is a disagreement (depending on wavelength) between the results of the present experiment and those of the other observers referred to. Fig. 10A reveals this disagreement in a tendency for points from the green to fall higher than those from the blue.

Fig. 10B differs from Fig. 10A in that the points representing multiplets have been shifted vertically to correct for the discrepancy discussed in Sect. A. The correction is an average one (See Pp. 52-54) and should be used between just two wavelengths, one, $\bar{\lambda}_b$, representing the average wavelength of the blue lines used, and the other, $\bar{\lambda}_g$, representing the average wavelength of the green lines used. For blue multiplets whose lines of known gf-value are at an average wavelength, $\bar{\lambda}_m$, at least 25A from $\bar{\lambda}_b$, and for green multiplets where $\bar{\lambda}_m$ and $\bar{\lambda}_g$ differ by 25A, the correction factor was altered assuming that it followed the equation,

$$\text{Correction factor} = \frac{1.8}{\bar{\lambda}_g - \bar{\lambda}_b}(\bar{\lambda}_g - \bar{\lambda}_m) = \frac{1.8}{900}(5260 - \bar{\lambda}_m).$$

The choice of 25A as the minimum separation of $\bar{\lambda}_m$ and $\bar{\lambda}_g$ or $\bar{\lambda}_b$ implies a maximum uncertainty in the correction factor of 3 per cent, which is less than the uncertainty already present in each point of Fig. 10A.

The interpretation of the distribution of points seen in Fig. 10B is critical, and will be considered now. If each line in the spectrum of the iron arc obeyed Eq. (1), with 4100°K, each point in Fig. 8 would fall on the straight line there drawn. If some lines were self-absorbed, the points in Fig. 10B would fall below the temperature-line; but because of the way in which Fig. 10B is plotted from the results of Fig. 9, the points in Fig. 10B would still fall on the ϵ_m axis. If, further, some multiplets were self-reversed, then the measured lines of each multiplet self-reversed would give points each lying the same distance, a, below the straight line in Fig. 8; and each self-reversed multiplet would be represented by a point in Fig. 10B, a units below the axis. Self-reversal, measured by the parameter a, would be expected to increase as multiplets of decreasing lower term excitation potential were studied.

The points in Fig. 10B do not have the expected positions. If there is any self-reversal, it is completely masked by other, unknown, effects. A search for these effects was initiated, in which the following possibilities were investigated:

1. Some experimental error was suspected, for the signal strengths involved in the calibration run and in

the iron arc run were different. In general, the comparison signal v'' and the maximum scanned signal v' were stronger in the case of the arc spectrum. Thus a ratio of $F_0=0.5$ could result from the comparison of $v'=0.7$ volts with $v''=1.4$ volts in the case of the arc, and of $v'=0.2$ volts with $v''=0.4$ volts for the lamp spectrum. This situation strongly suggests that the instrument gave incorrect ratios because of the effect already discussed on Pp. 29-31. Some trial calculations were carried out in which the ratios given by the instrument were corrected for the effect described on Pp. 29-31. It was found that the corrections did not begin to reduce the configuration of points on Fig. 10B to a form such as that discussed on P. 59.

2. It has been stated that a comparison of the present data with those of Crosswhite showed (a) that the arcs used had a different temperature, and (b) that our green lines were too bright (P. 53). The two sets of data were compared again, in a way which corrected for these two differences, and the result was a confirmation of the configuration of points in Fig. 10B.

3. It has been pointed out that the results of this experiment are also too bright for green lines on the basis of the work of King and Carter (P. 53).

This discrepancy has been corrected for in Fig. 10B, and hence the distribution of points represent a further disagreement with those observers. An attempt was then made to find whether the disagreement was one with the data of King or with those of Carter. The curves of Fig. 9, and therefore the points of Fig. 10B, are not changed significantly if only those spectrum lines are used for which gf-values were measured by one observer.

These last three comments lead to the conclusion that Fig. 10B describes a real effect which occurs in the arc but not in the furnace. Physical meaning for the effect was sought in these further investigations:

4. Some connection with the odd-even effect discovered by Carter (P. 2) was sought, but no correlation was evident.
5. An attempt was made to relate the ordinates of the points in Fig. 10B with the electronic configurations of the upper terms of the multiplets. Again, no correlation was observed.

D. Corrections to Existing gf-values

In the plotting of Fig. 8 and Fig. 9 it was found that several lines were consistently too faint or too bright relative to other lines in the same multiplets on the basis of the gf-values which had been measured for them by Carter (16). The extent of the correction necessary was in each case read off a graph like Fig. 9, and is presented in Table IA.

It was concluded in the previous section that some effect appears in operation in the iron arc which is absent in the furnace; and that this effect causes the points in Fig. 10B to differ from the positions along the $\mathcal{E}_m$ axis which they would otherwise have. In Table IB gf-value differences are given, which, if applied to the gf-value of each line which was measured in the multiplets listed, would move the point representing that multiplet to the $\mathcal{E}_m$ axis; the values listed are the ordinates (absolute value) of the points now appearing in Fig. 10B. The gf-value differences are such as to allow the measured relative iron line intensities to obey Eq. (1), except for the effect of self-absorption. The manner in which these terms were read from Fig. 10B means that the wavelength-discrepancy with the data of King and Carter is not inherent in the terms.

E. Temperatures for Different Arc Conditions

The approximate independence of temperature over a large range of current has been reported by Duffendack and La Rue (11) and by others; Ornstein, Brinkman and Beunes (34) report a decrease of arc temperature as the air pressure is reduced below 1 atmosphere. These groups both used photography.

The results of measurements of the temperature of the arc at different currents and pressures, and in different portions of the arc, are presented in Table II.

The inverted image of the arc on the slit was about 16 mm high, and equally broad. The slit was 3 mm high and in most cases 0.75 mm broad. The "edge" of the arc is defined as that region on the arc equator which marks the outer limit of the blue core of the arc; the "positive pole" and "negative pole" regions are on the axis of the arc and are bounded by the pole or the bead on the pole.

In each of the runs from which these data were obtained, the reduction of the data and the presentation of results proceeded as before, up until the plotting of points on a graph like Fig. 8. The determination of a temperature was again made by fitting the points with a straight line, but now the slope of the straight line was predetermined by the requirement that it pass above or below each point (not representing a weakened line) by the same amount as in the case of the standard arc. This requirement was consistently met

for all the different cases studied. So the tendency of certain multiplets to vary, as whole groups of lines, from the intensities calculated by Eq. (1), which has been exhibited in Fig. 10B, is not sensitive to the arc current, to the pressure of the air in which the arc runs, and to the part of the arc studied. The effect of Fig. 10B, then, though perhaps due to the peculiar conditions in the arc, is not sensitive to changes in arc conditions.

F. Self-absorption for Different Arc Conditions

The self-absorption found in the standard arc was described and compared with the theory of Cowan and Dieke on P. 56. The prediction that increasing current will increase self-absorption has also been found correct.

Fig. 11 shows the changes of self-absorption with changing conditions; the curves have, for comparison purposes, been shifted up and down from the positions they would otherwise occupy (compare Fig. 9) to a common level. Fig. 11 shows that the amount of self-absorption increases with the current and with the pressure. The same amount of self-absorption is present in all parts of the arc.

G. Summary of Results

The purpose of this experiment has been to explore the excitation conditions in the iron arc by studying those emission lines for which gf-values have been measured in furnace spectra, and in this way to establish whether the arc is a suitable source for further measurement of gf-values.

It appears that when the effects of self-absorption and self-reversal are absent or corrected for, a single excitation temperature can be assigned to the arc on the basis of an assumption of a Boltzmann distribution of atoms in the upper states of the transitions producing the lines.

Self-absorption affects strong lines and lines of low excitation. For an arc operating at atmospheric pressure and on 2.3 amps, the effect is negligible for all lines whose lower term at least 2.1 volts (a^5P): for an arc at 4 cm of Hg and 3.5 amps, the effect can be neglected for all lines whose lower terms are at least 1.5 volts.

The temperatures in various parts of the arc differ little. The changes of temperature which result when current and pressure are changed are also small.

The temperature of the arc is 4100°K. This excitation temperature exceeds that produced by the furnace.

There is an unexplained difference, which is a function of wavelength, between the results of this experiment and those of two others. This difference must be explained.

There is a further difference which appears to be one due to some mechanism in the arc which is absent in the furnace spectra. Whole multiplets of measured lines are too strong or too weak to fit the Boltzmann distribution of atoms in the upper state. Some non-equilibrium mechanism is suspected but was not found. Further investigation should be made.

So the arc appears to be a promising source for future measurements of gf-values, providing the measurements are confined to relatively weak, high level lines.

BIBLIOGRAPHY

1. King, R. B., "Relative gf-values for Lines of VI," Astrophys. J., 105, 376, 1947.
2. King, R. B., "Relative gf-values for Lines of NiI," Astrophys. J., 108, 87, 1948.
3. King, R. B., "Absolute f-values for Lines of FeI; Abundance of Fe in the Sun," Astrophys. J., 95, 78, 1942.
4. King, R. B., and King, A. S., "Relative f-values for Lines of FeI and TiI," Astrophys. J., 87, 24, 1938.
5. Smit, J. A., "The Determination of Temperature from Spectra," Physica, 12, 420, 1947.
6. Korf, S. A., and Breit, G., "Optical Dispersion," Rev. Mod. Phys., 4, 427, 1932.
7. Unsöld, A., "Quantitative Spektranalyze der Sonnenatmosphäre," Zeit. f. Astrophys., 24, 306, 1948.
8. Aller, L. H., Astrophysics: the Atmosphere of the Sun and Stars, Ronald Press, New York, 1953.
9. McCann, Conner and Ellis, "Dielectric Recovery Characteristics of Power Arc in Large Air Gaps," Am. Inst. Elec. Eng. Trans., 69, 1950.
10. Watts, Evans, and Lloyd, "Flame Travel in and Internal Combustion Engine," Engineering, P. 713, 1937.
11. Duffendack, O. S., and La Rue, J. M., "Temperature in Spectroscopic Sources Used in Analytical Work," J. Opt. Soc. Am., 31, 146, 1941.

12. Hemmendinger, H., "Electrode Concentrations and Total Intensity of Spectrum Lines," J. Opt. Soc. Am., 31, 150, 1941.

14. King, R. B., "Temperature in the Solar Reversing Layer from Ti Lines," Astrophys. J., 87, 40, 1938.

15. Wilson, O. C., "Structure of the Atmosphere of the K-type Component of Aurigae," Astrophys. J., 107, 126, 1948.

16. Carter, W. W., "Measurements of f-values in the Iron Spectrum with Applications to Solar and Stellar Atmospheres," Phys. Rev., 76, 962, 1949.

17. Cowan, R. D., and Dieke, G. H., "Self-absorption of Spectrum Lines," Rev. Mod. Phys., 20, 418, 1948.

18. Richtmeyer, F. K., and Kennard, E. H., Introduction to Modern Physics, McGraw-Hill, New York, 1947.

19. Jenkins, F. A., and White, H. E., Fundamentals of Physical Optics, Pp. 36 and 37, McGraw-Hill, New York, 1937.

20. Mitchell, A. C. G., and Zermansky, M. W., Resonance Radiation and Excited Atoms, MacMillan, New York, 1934.

21. Crosswhite, H. M., "Photoelectric Intensity Measurements in the Iron Arc," Spectrochimica Acta, 4, 122, 1950.

22. Harrison, George R., "Intensity Relations in the Spectra of Titanium," J. Opt. Soc. Am. (and Rev. Sci. Instr.), 17, 389, 1928.

23. Bredt, Irene, "Grundsatzliches uber Spektroscopische Verfahren zur Messung von Temperaturen und Geschwindigkeiten sehr Schnell Stromerides Fenergase," Zeit. f. Elektrochemie, 56, 71, 1952.

24. Mannkopf, R., "Uber Elektrondicht und Elektrontemperature in Frei Brennenden Lichtbögen," Zeit. f. Phys., 86, 161, 1933.

25. Ornstein, L. S., and Brinckman, H., "Der Thermische Mechanismus in der Säule des Lichtbogens," Physica, 1, 797, 1934.

26. Penner, S. S., and Bjönerud, E. K., "Experimental Determination of Rotational Temperatures and Concentrations of OH in Flames from Emission Spectra," Jet Propulsion Laboratory, California Institute of Technology, Technical Report # 14, June 1954.

27. Engstrom, R. W., "Multiplier Phototube Characteristics," J. Opt. Soc. Am., 37, 420, 1947.

28. Huldt, Lennart, "Determination of Excitation on Energies of Atoms with Phototubes and Oscillograph," Arch. f. Phys., 2, 353, 1950-1.

29. Kessler and Wolfe, "The Measurement of Intensity Ratios of Spectral Lines with Electron Multiplier Phototubes," J. Opt. Soc. Am., 37, 133, 1947.

30. Brown Instrument Division, Minneapolis-Honeywell Regulator Company, "Characteristics of Measuring Circuits in Brown Electronik Potentiometers," Bulletin N. B15-13, 1951.

31. Stout, M. B., Basic Electrical Measurements, Pp. 69 f., Prentice-Hall, New York, 1951.

32. Potter, E. V. and Scott, A., "An Automatic Arc-current Regulator," Rev. Sci. Instr., 18, 722, 1947.

33. Forsythe and Worthing, "The Properties of Tungsten and the Characteristics of Tungsten Lamps," Astrophys. J., 61, 146, 1925.

34. Ornstein, L. S., Brinkman, H., and Beunes, A., "Prufung der Comptonschen Bogentheorie durch Messung der Bogengastemperature als Funktion des Druckes," Zeit. f. Phys., 77, 72, 1932.

APPENDIX I

(Referred to on P. 35 and P. 55)

Investigations into the Possibility of Significant Experimental Differences Between the Standardization Run on the Lamp, and the Iron Arc Run, which Would Result in Systematic Error.

1. An aluminum-coated first-surface mirror was used for (D) in Fig. 7. This mirror reduced the color temperature of a source at 2290°K by only 60°K with a 45° angle of incidence. And this decrease was applied to the measured pyrometer temperatures on all data obtained by the use of the mirror.
2. If large wavelength differences had been encountered in this experiment, the lens (B) in Fig. 7 might, in focusing the arc and the lamp filament (which are of different shapes) on the slit, lose light of long or short wavelengths in one or the other case due to chromatic aberrations. However, the lens is achromatic and the spectrum region observed is short, so that no such effect could enter significantly.
3. It has already been said on P. 29 that scattered light (which would behave differently in the cases of the arc and the lamp) is at most a negligible effect.

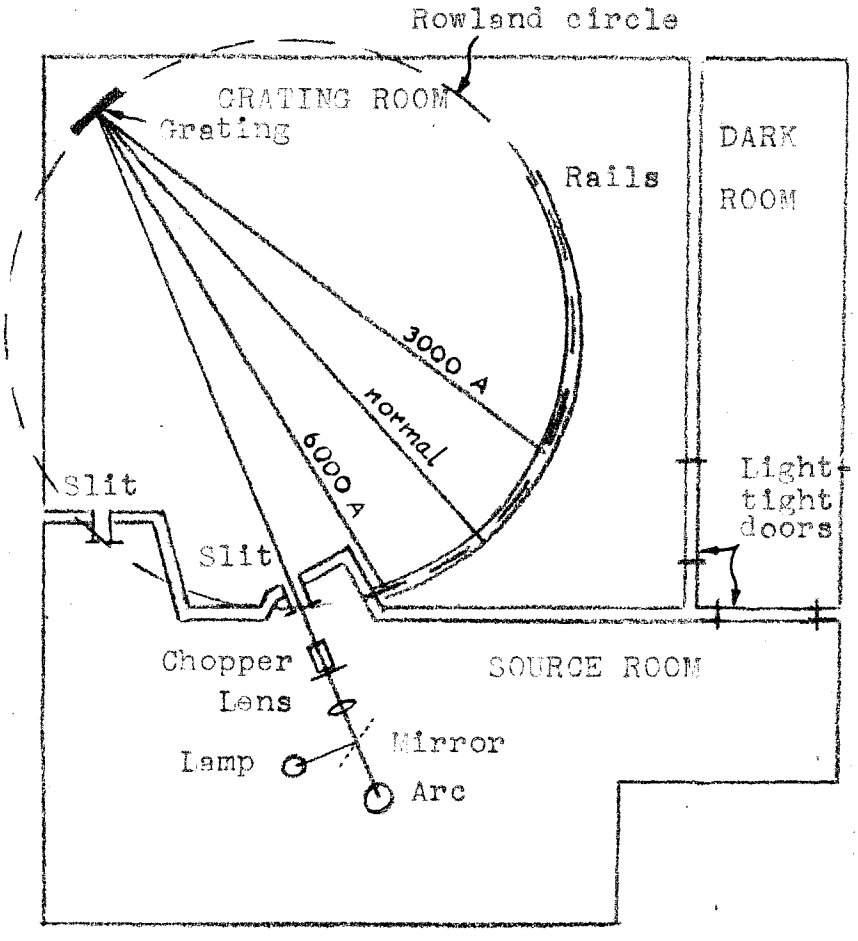

FIGURE 1

Layout of Apparatus.

(Not to scale)

KEY TO SYMBOLS OF FIG. 2

(A) Main portion of carriage

(B) Rack which determines orientation of assembly (C) and also allows driving of carriage by motor (F)

(C) Top assembly for slit and photocell unit

(D) Exit slit

(E) Focus adjustment

(F) Driving motor

(G) Finder prism

(H) Finder lens

(I) Photocells

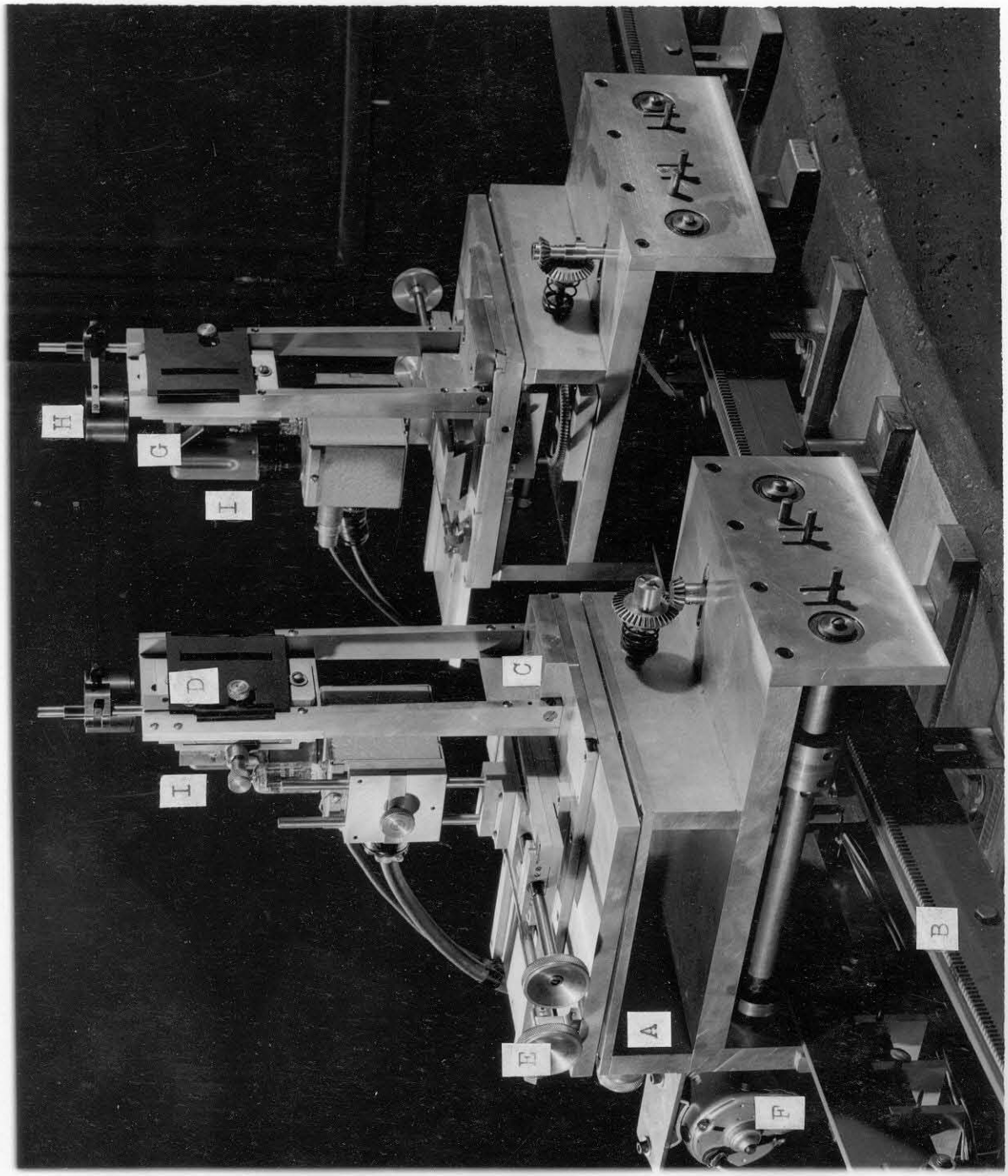

FIGURE 2

Photocell Carriages
On Spectrograph Rails

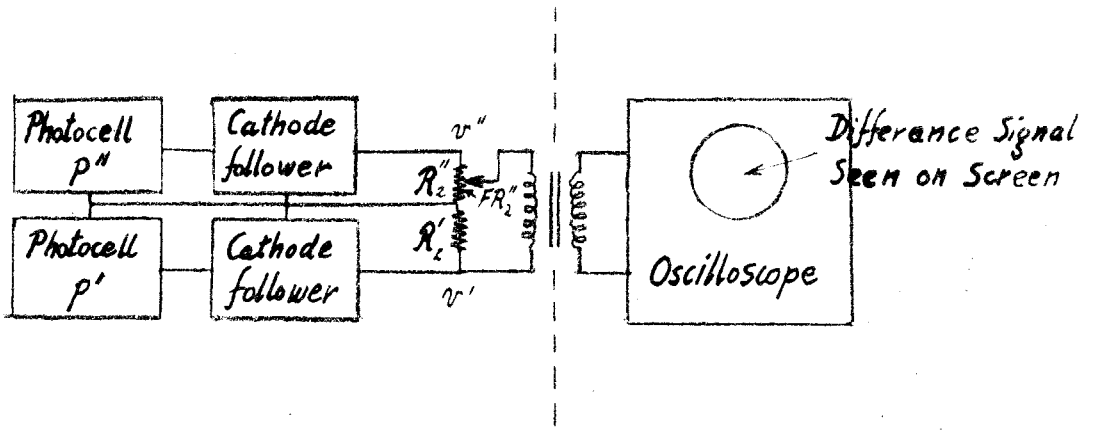

FIGURE 3

Use of Oscilloscope to Show Difference of Cathode Resistor signals. Slider of Potentiometer Moved by Hand Until Pattern on Screen Reduces to a Line

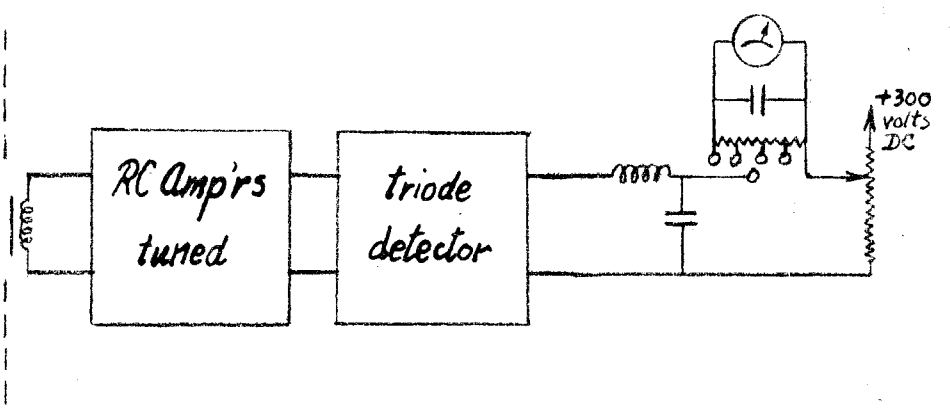

FIGURE 4

Meter to Indicate Off-Balance of Instrument. All to Left of Dotted Line Is the Same as in Fig. 3

PARTS LIST - SEE FIG. 5

S_1 DPDT Switch, interchanges photocell units

S_2 DPDT Switch, for observing signals on oscilloscope

R_1 10 k, cathode resistor

R_2 10 k, wirewound potentiometer, cathode resistor

R_4 100 k, bleeder for 6AK6 grid bias

R_5 39 k, bleeder for 6AK6 grid bias

R_6 10 meg, load resistor for photocell

R_7 0.8 meg, dynode bleeder

R_8 2.8 meg, dynode to ground

C_1 4 μf, DC blocking condenser

C_2 150 $\mu\mu f$ max. trimmer condenser, adjust phase of v

T UTC # LS-50; hum attenuation -74 db, turns ratio 3 when connected as follows:

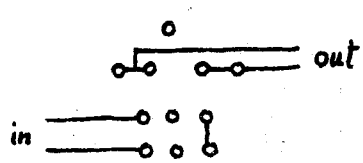

NOTES ON FIG. 5

The diagrams do not show the following:

1. 300 volt DC plate power supply, which is a standard circuit.
2. 900 volt DC photocell power supply. This consists of batteries, each 67 volts, in series, contained in an electrostatically shielded wooden box. A 4 μf condenser is connected across the batteries to shunt out any hum pickup.
3. The 6 volt DC filament supply, an automobile battery.
4. The care with which grounds were placed to avoid ground loops.
5. Assorted meters and switches.

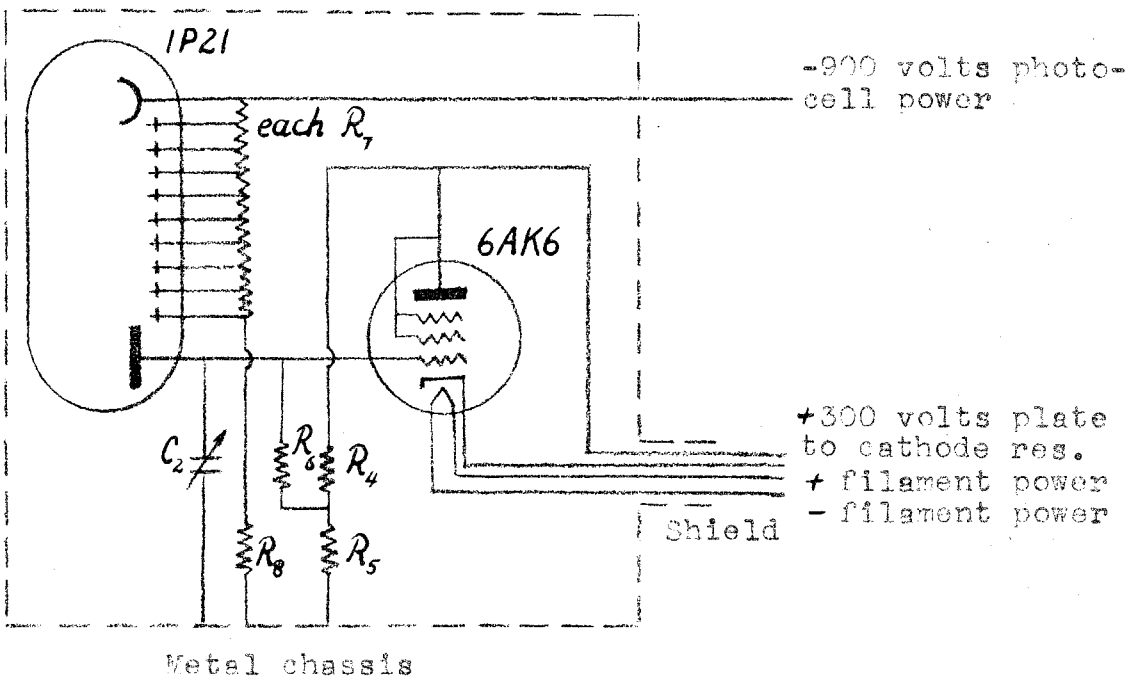

FIGURE 5a

Circuit of Photocell Units.

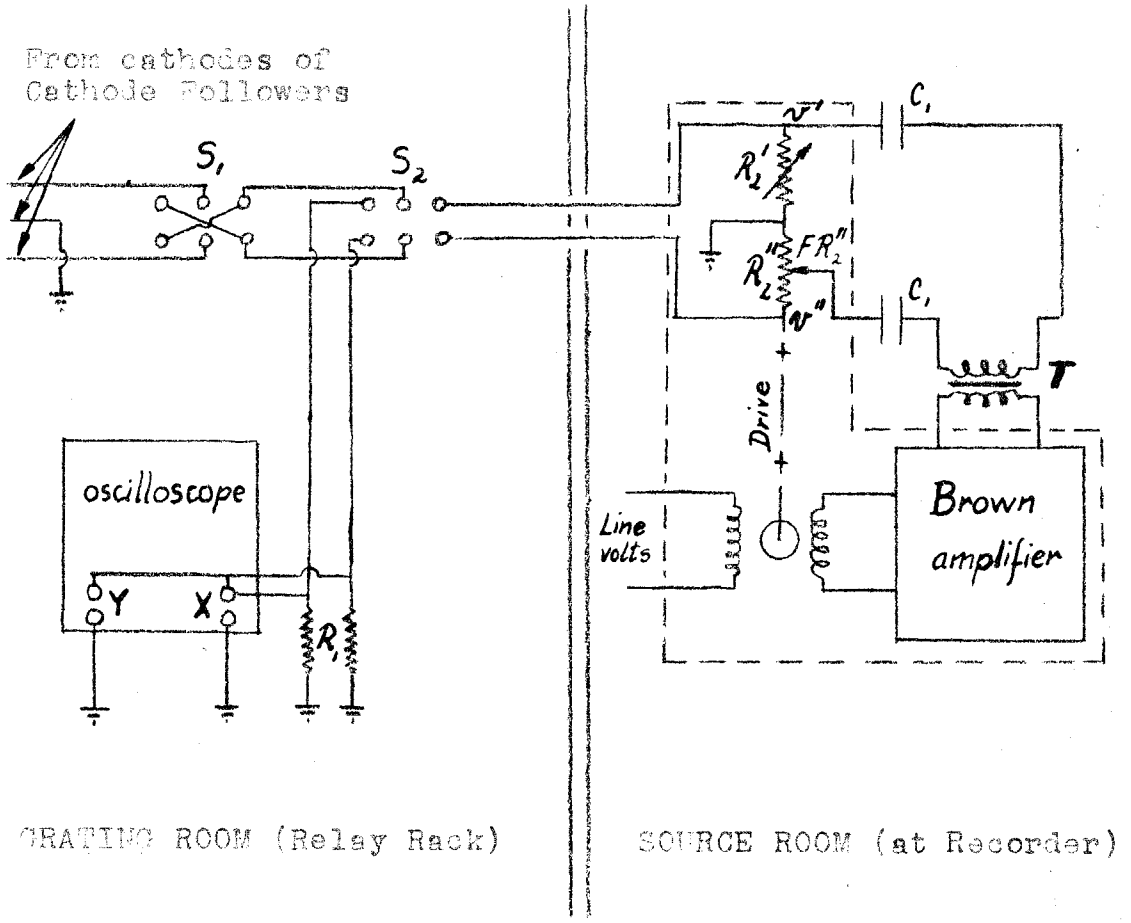

FIGURE 6b

Overall Wiring Diagram.

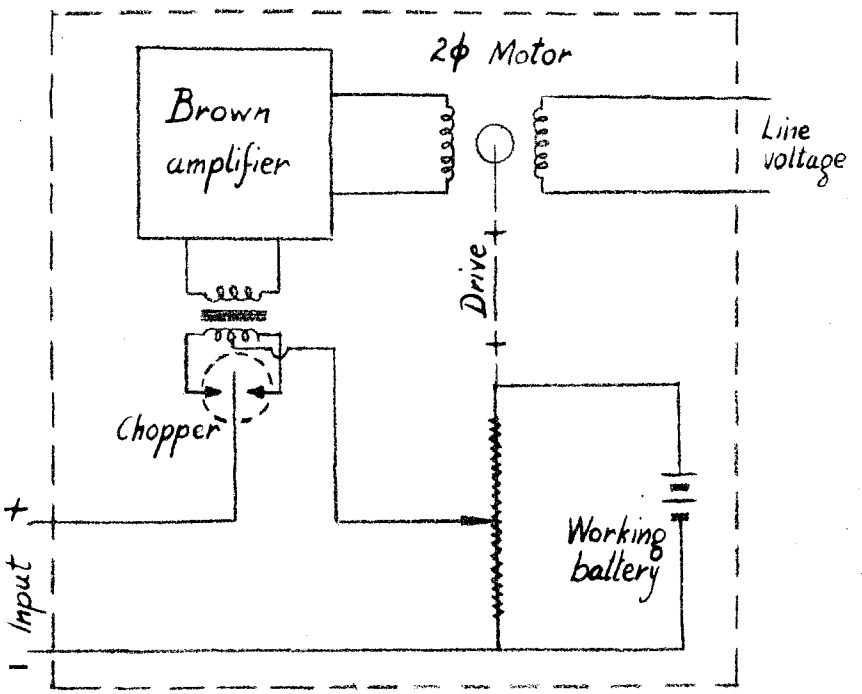

FIGURE 6

Schematic Circuit Diagram of Brown Recorder for use in DC Voltage Measurements

(See Ref. 30.)

KEY TO SYMBOLS ON FIG. 7

(A) Stand provides motion for adjustment of arc position

(B) Lens

(C) Chopper

(D) Mirror which can be inserted to send light from lamp (E) into the spectrograph

(E) Tungsten ribbon filament lamp

(F) Arc chamber

(G) Optical pyrometer

(H) Slit

(J) Adjusts top electrode.

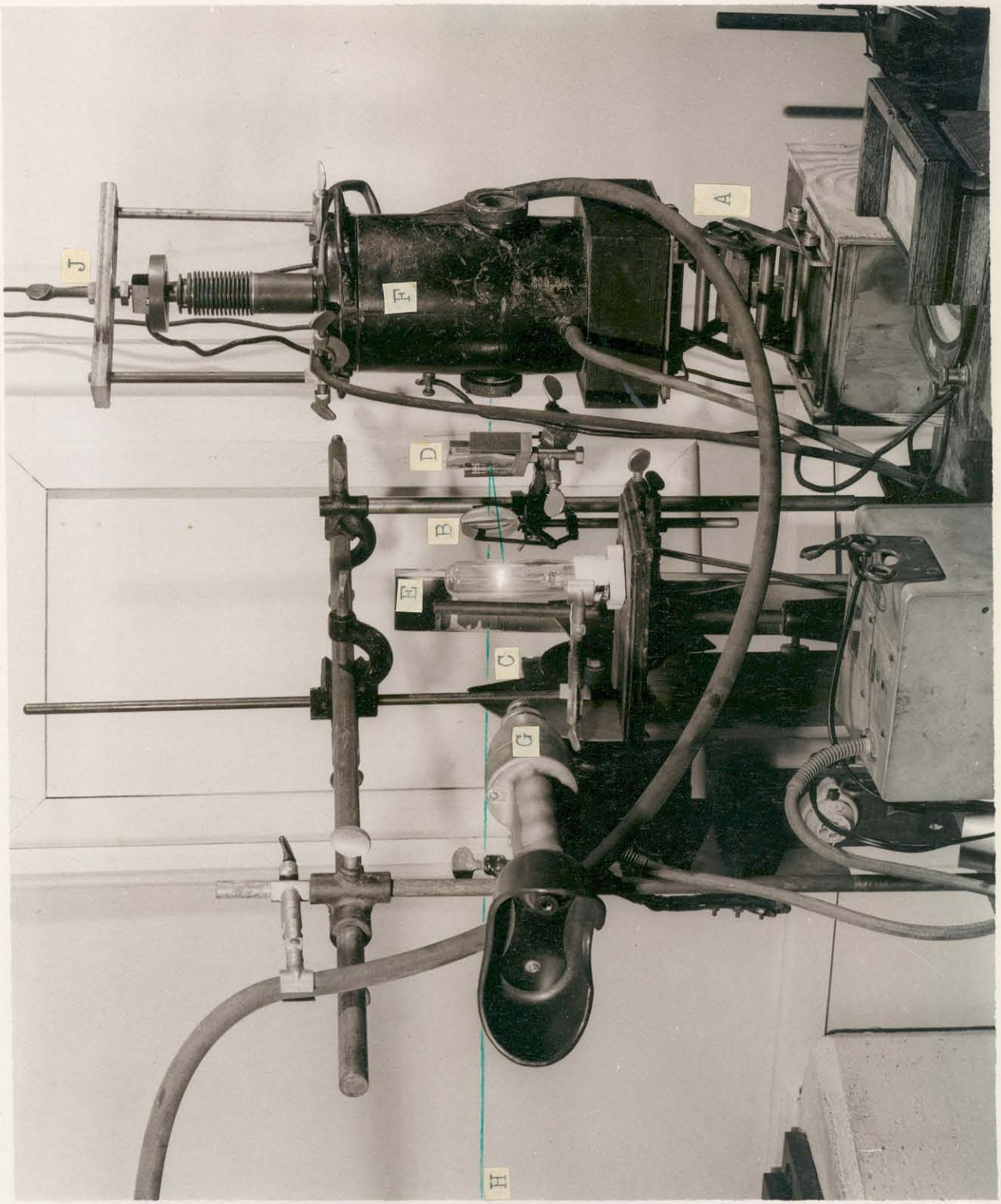

FIGURE 7

Arrangement of
Apparatus in Source Room

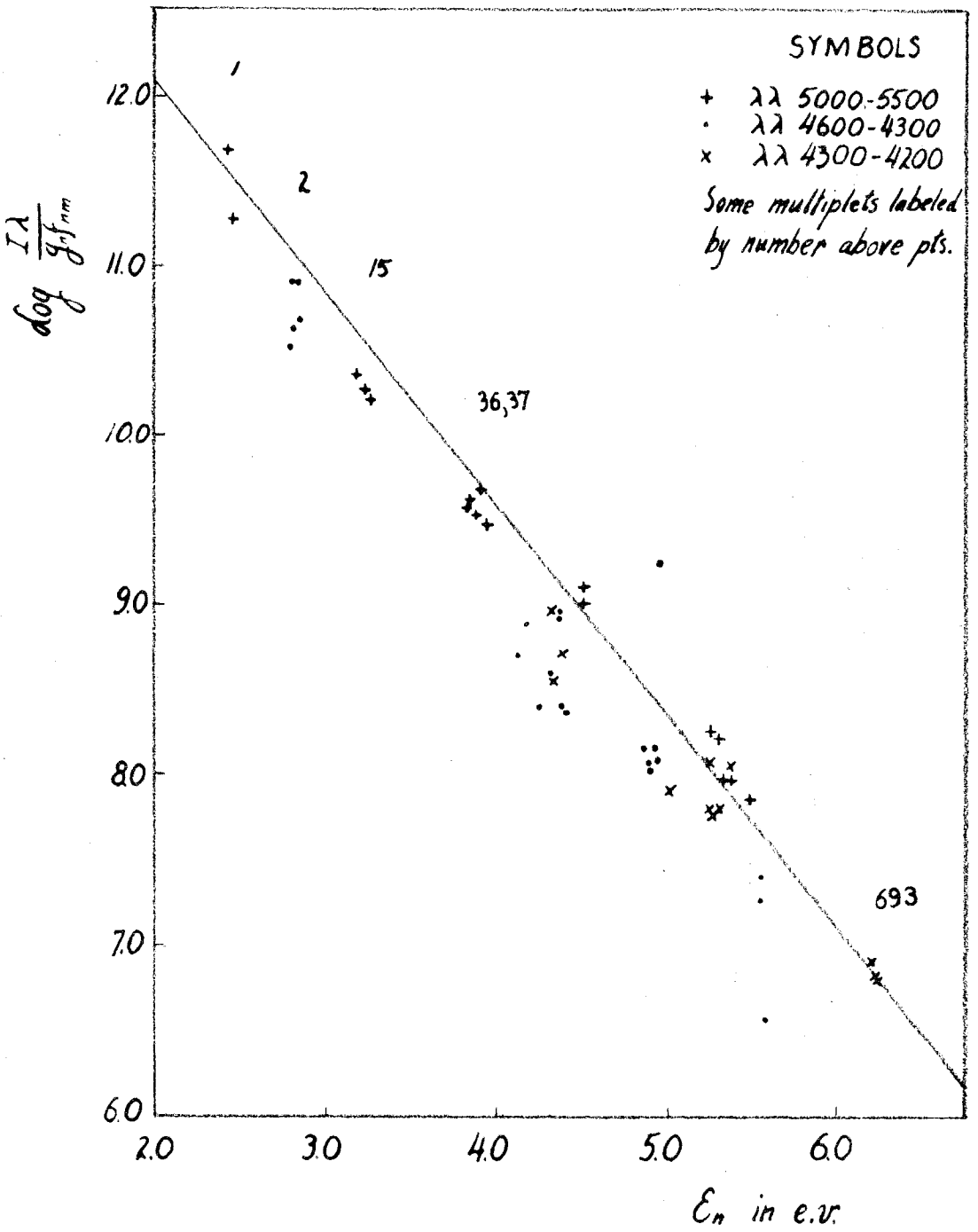

FIGURE 8

Graph for Determination of Temperature at Center of the Arc Running with Pressure 1 Atmosphere and Current 2.5 Amperes (Standard Conditions).

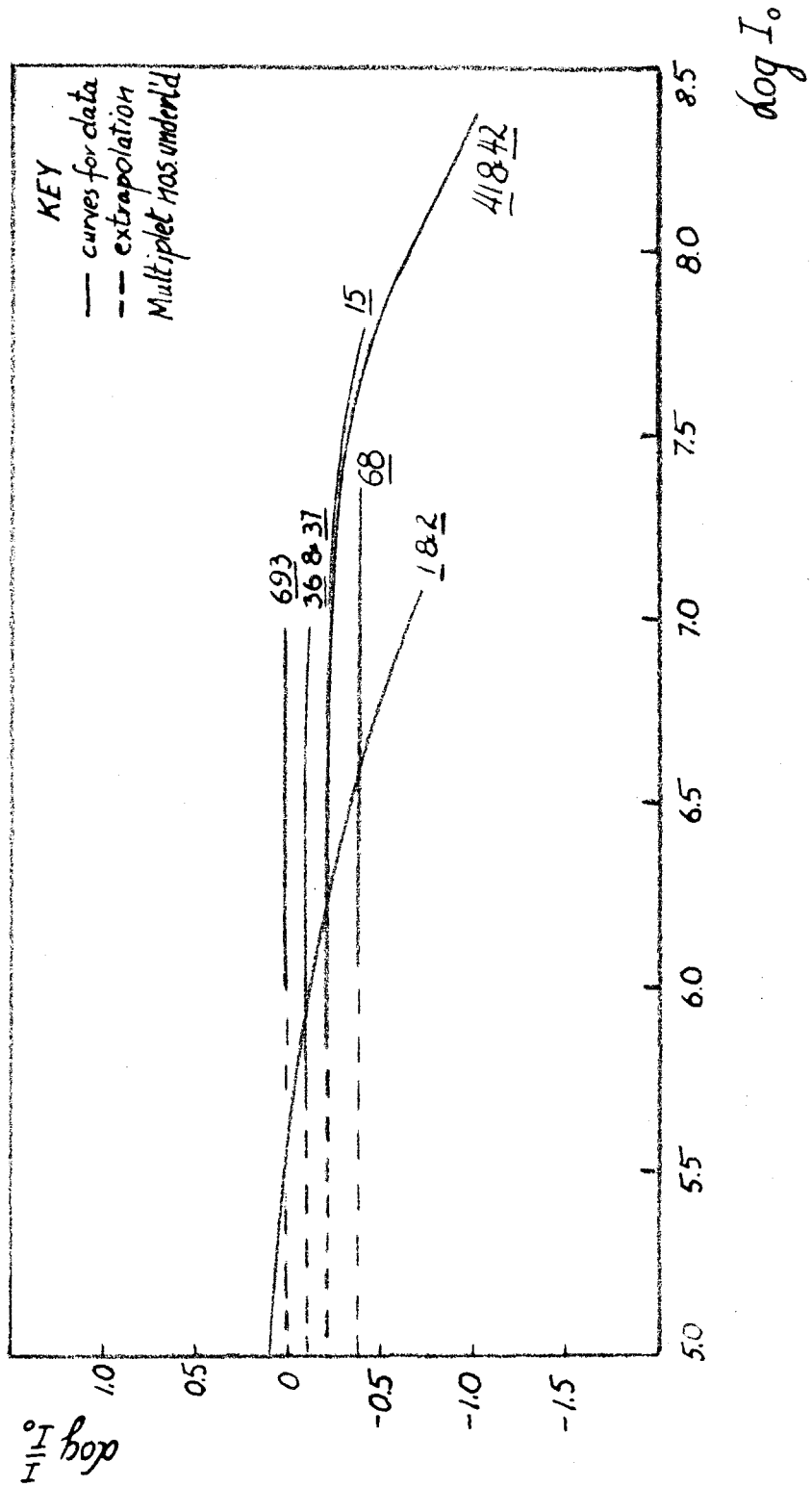

FIGURE 9

Graph for Determination of Self-absorption and Self-reversal for Lines of Selected Multiplets in the Iron Spectrum for the Standard Iron Arc

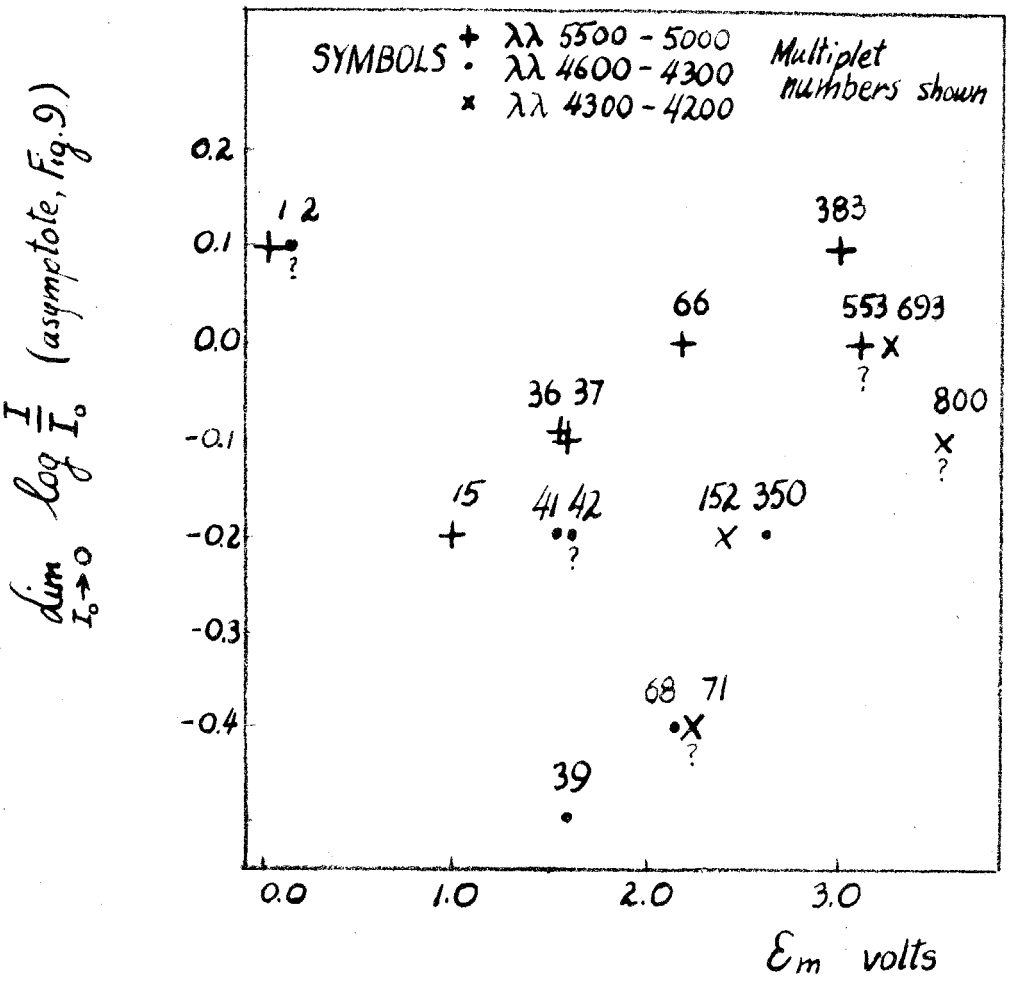

FIGURE 10A

Showing the Tendency of the Intensities of All Lines in Multiplets to Differ from the Intensities Calculated from Eq. (1')

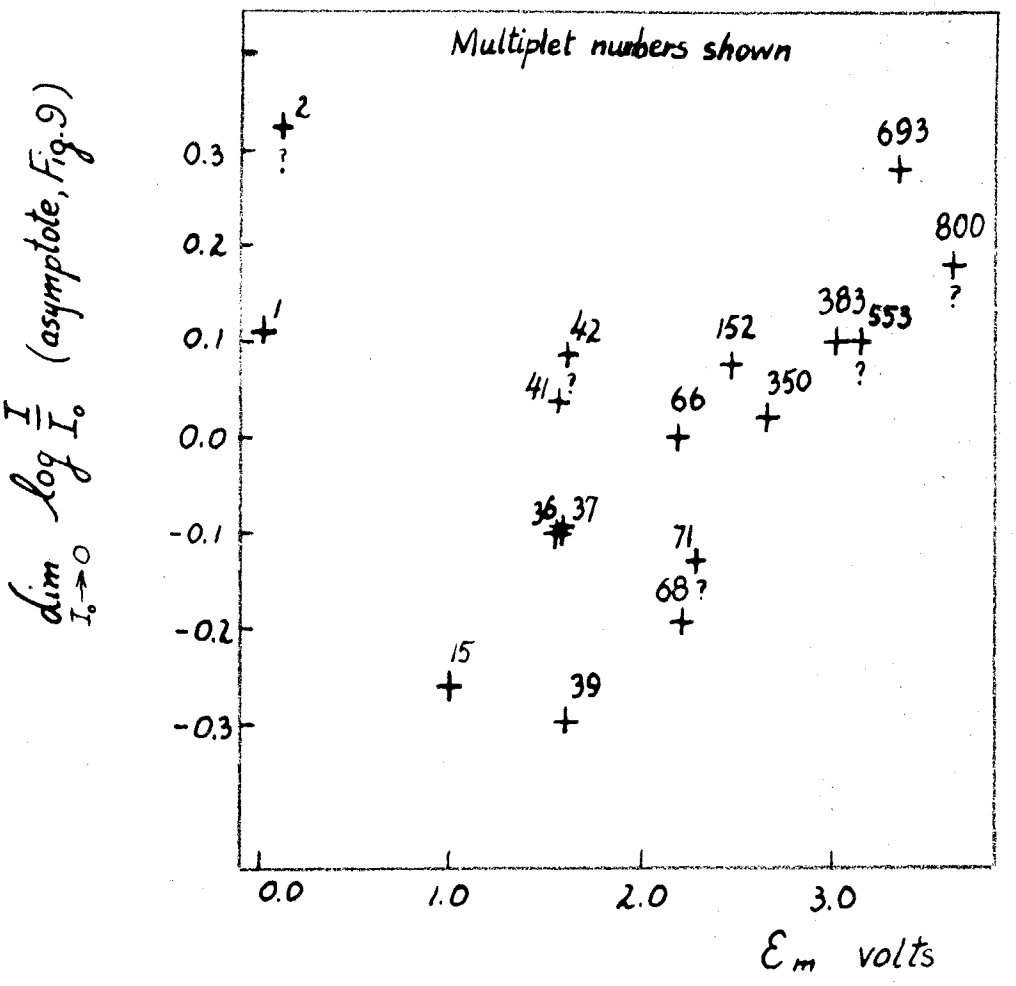

FIGURE 10B

Same as Fig. 10A but Points Have Been Moved to Correct for Wavelength-Dependent Error. Points Not Sorted by Wavelength Region

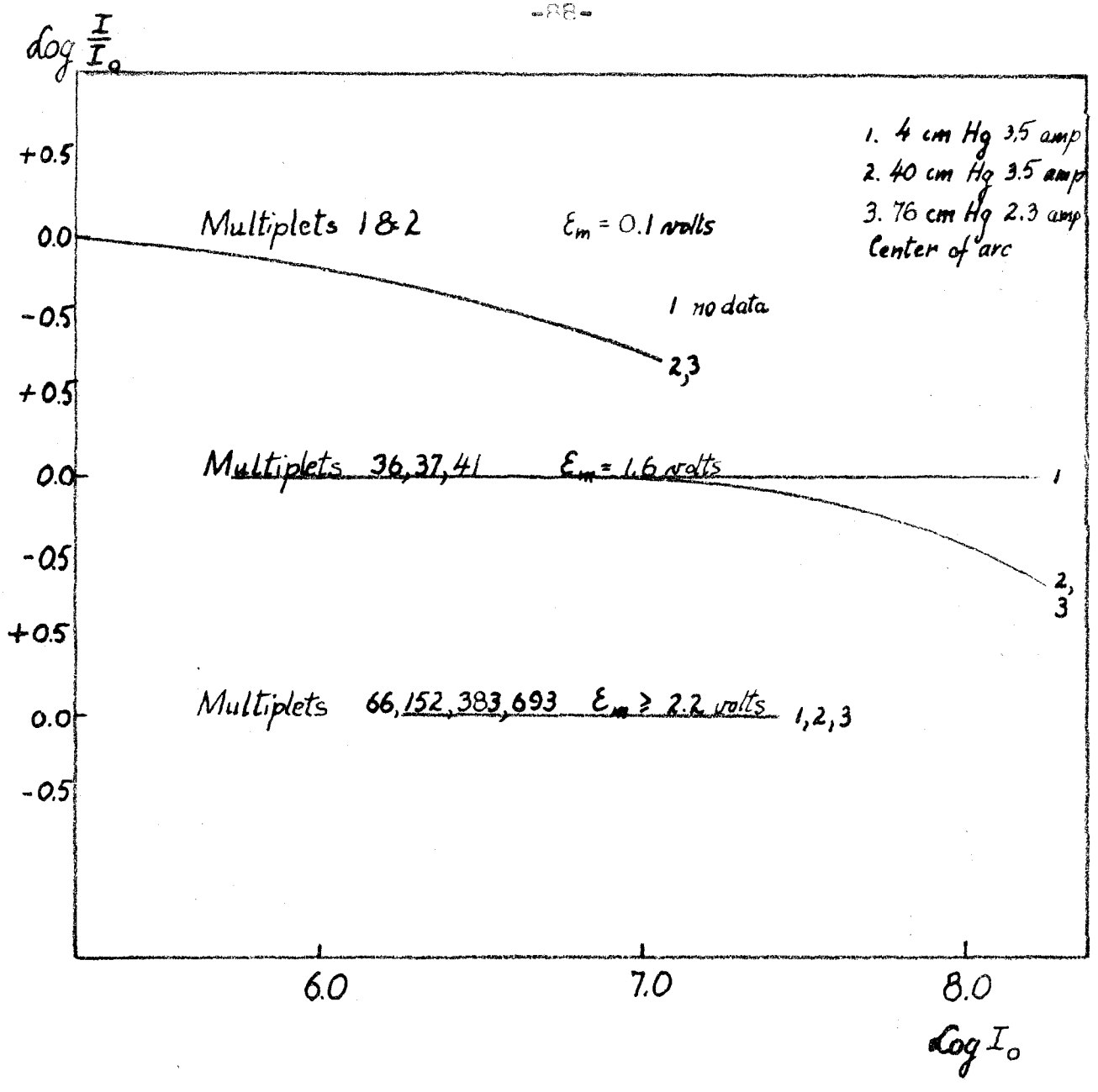

FIGURE 11A

Self-absorption Effects as They Depend on Pressure. Curves Are Plotted Following Eq. (2). Curves Have Been Shifted for a Given $\mathcal{E}_m$ to a Common Level (Compare Fig. 9) for Comparison Purposes.

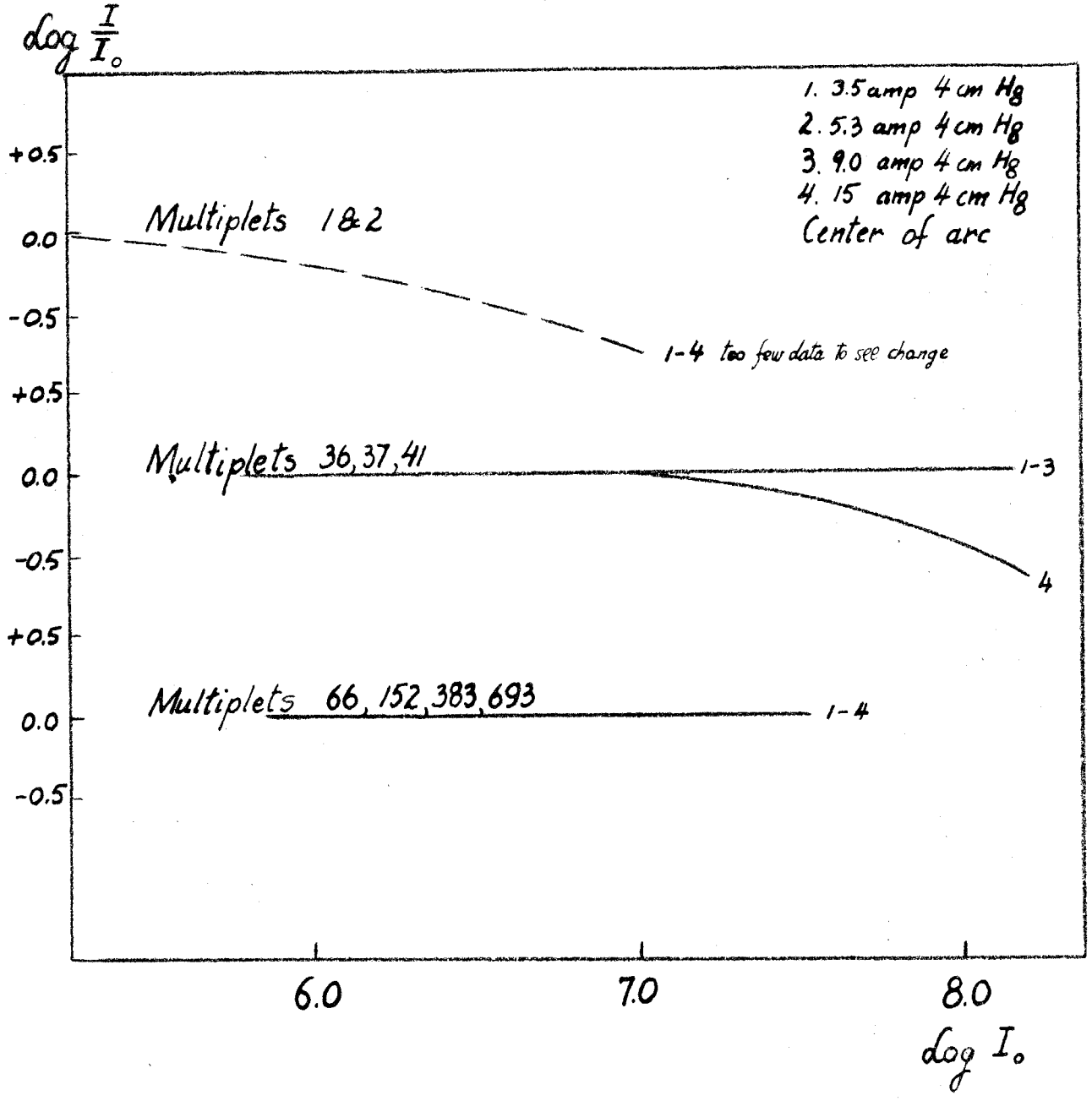

FIGURE 11B

Self-absorption Effects as They Depend on Pressure of Air

TABLE IA

Corrections to gf-values of Carter (16) for Certain Lines, Relative to the gf-values of Other Lines in the Multiplets to Which the Lines Belong

λ	Multiplet	Listed gf-value	Corrected gf-value
4299	152	2120	3400
4431	68	22	270
4443	350	12570	1257
4454	350	2470	1000

TABLE IB

Instrument Ratios for Lamp Spectrum, Arc Intensities, Ordinates for Fig. 8, and gf-value Differences, for Lines of the Standard Arc Arranged According to Multiplet Number and Wavelength

Mult. Number		Ratio for Lamp Spectrum	Arc Int.	Ordinate of Fig. 8	gf-value* Difference
1	5247	4.80	0.09	11.68	-0.1
	5204	4.53	0.34	11.28	-0.1
2	4490	1.07	0.34	11.18	-0.3**
	4482	1.05	0.96	11.03	-0.3**
	4462	1.00	0.92	10.75	-0.3**
	4427	0.90	1.02	10.63	-0.3**
	4376	0.77	1.04	10.60	-0.3**
15					
15	5405	6.09	1.62	10.03	≠0.35
	5397	6.09	1.56	10.36	≠0.35
	5371	5.93	1.80	10.13	≠0.35
36	5332	5.35	0.29	9.63	≠0.1
	5307	5.16	0.22	9.69	≠0.1
	5216	4.62	0.88	9.50	≠0.1
37	5341	5.43	1.06	9.54	≠0.1
	5171	4.34	1.26	9.60	≠0.1
39	4602	1.53	0.59	8.78	≠0.3
	4531	1.20	0.72	8.91	≠0.3
41	4415	0.86	1.78	9.06	-0.05
	4404	0.82	1.95	8.71	-0.05
	4383	0.79	2.04	8.49	-0.05
	4337	0.72	0.95	8.95	-0.05
	4294	0.66	1.44	8.96	-0.05
42	4326	0.70	1.86	8.54	-0.1**
	4307	0.67	1.81	8.51	-0.1**

Table IB Continued

	4272	0.64	1.80	8.60	-0.1**
	4202	0.51	1.62	8.74	-0.1**
66	5251				
66	5251	4.83	0.55	9.12	0.0
	5202	4.52	0.70	9.02	0.0
68	4528	1.20	1.33	8.18	∕0.2
	4494	1.08	1.03	8.09	∕0.2
	4459	1.00	0.95	8.07	∕0.2
	4447	0.94	0.82	8.12	∕0.2
	4442	0.93	0.89	8.23	∕0.2
	4430	0.90	0.48	9.27	∕0.2
71					
71	4282	0.65	1.19	7.93	∕0.1**
152	4299	0.67	1.32	8.10	-0.1
	4271	0.64	1.33	7.80	-0.1
	4260	0.63	1.69	7.87	-0.1
	4236	0.61	1.38	7.79	-0.1
	4233	0.60	1.38	8.02	-0.1
350	4476	1.05	0.65	7.41	0.0
	4454	0.96	0.52	7.28	0.0
	4443	0.93	0.54	6.59	0.0
383	5266	4.94	1.28	8.23	-0.1
	5233	4.72	1.61	8.25	-0.1
	5192	4.46	1.21	8.00	-0.1
	5191	4.46	1.04	8.00	-0.1
553	5324	5.30	1.35	7.88	- .1**
693	4247	0.61	0.76	6.85	-0.3
	4238	0.61	0.79	6.82	-0.3
	4227	0.58	1.17	6.90	-0.3
800	4216				-0.2**
n=n (Fig. 8)					***

** Douhtful because only one line in multiplet or because of too much scatter.

* This column gives the negative ordinates of the points in Fig. 10B. Therefore the wavelength-dependent discrepancy with the data of other observers has been omitted in the entries. Entries are 0.03.

*** Evaluated from runs over other arc conditions.

TABLE IIA

Temperatures at the Center of the Iron Arc Operating Under Different Conditions

Air Pressure in cm of Hg	Current in Amperes				
	2.3	3.5	5.3	9.0	15
4		4600*	4600	4600	4100
40		4100		4100	
76	4100**				

* All entries in ^{o}K
** Standard Arc

TABLE IIB

Temperatures at Various Parts of the Arc for a Given Current (3.5 amps) and Pressure (40 cm Hg)

Part of Arc	Temperature (^{o}K)
Center	4100
Either edge	4100
Negative pole	4450
Positive pole	4450